PAGEOPH, Vol. 134, No. 3 (1990) 0033–4553/90/030355–30$1.50 + 0.20/0

M_m: Extension to Love Waves of the Concept of a Variable-period Mantle Magnitude

EMILE A. OKAL[1] and JACQUES TALANDIER[2]

Abstract—We extend to Love waves the concept of the mantle magnitude M_m introduced recently for Rayleigh waves. Spectral amplitudes $X(\omega)$ of Love waves in the 50–300 s period range are measured on broad-band records from major events. A distance correction C_D, regionalized to reflect the influence of different tectonic paths, and a source correction C_S, compensating for the variation of excitation with period are effected; the exact geometry and depth of the event are however ignored. The resulting expression

$$M_m = \log_{10} X(\omega) + C_D + C_S - 0.90$$

is expected to be an estimation of $\log_{10} M_0 - 20$, where M_0 is the seismic moment of the event. All quantities in this equation are fully justified from a theoretical standpoint.

The analysis of a dataset of more than 300 Love records shows that M_m correctly describes the seismic moment, with average residuals in the range of 0.1–0.2 unit of magnitude. No significant trend with either distance or period of measurement is present. In particular, M_m does not saturate and continues to grow linearly with $\log_{10} M_0$ for very large events. The combination of the Rayleigh and Love M_m guards in general against underestimation of M_0.

Key words: Mantle magnitudes, Love waves, magnitude scales, tsunami warning.

1. Introduction and Background

The purpose of this paper is to extend to Love waves the mantle magnitude M_m introduced for Rayleigh waves by OKAL and TALANDIER (1989). In that study (hereafter "Paper I"), we showed that a real-time analysis of mantle Rayleigh waves could yield a reliable estimate of the moment M_0 of a teleseismic event, while keeping the basic principle of magnitude, i.e., ignoring the exact focal mechanism and true depth of the source.

On the basis of a large dataset of more than 250 records, we studied in Paper I the residuals between published values of the seismic moment (obtained mostly from the Harvard CMT files), and values estimated from the measurement of M_m at a single station. The standard deviation of such errors was found to be on the

[1] Department of Geological Sciences, Northwestern University, Evanston, Illinois 60208, U.S.A.
[2] Laboratoire de Géophysique, Commissariat à l'Energie Atomique, Boîte Postale 640, Papeete, Tahiti, French Polynesia.

order of 0.2 unit of magnitude. This figure is in itself excellent since it is comparable to the level of precision achieved by investigations of moment tensor solutions, and also to the scatter existing among measurements of classical magnitudes, such as M_s, at individual stations. However, the exclusive use of Rayleigh waves cannot guard against more significant errors in the unfavorable case of the station sitting in a fully developed node of radiation. The purpose of the present paper is thus to examine the extension of the M_m concept to Love waves, which should provide an alternative and a safeguard in such situations.

The structure of this paper follows closely that of Paper I. We refer the reader to that previous work, and will emphasize mainly those points characteristic of Love waves.

2. Theory

In direct parallel to the case of Rayleigh waves studied in Paper I, we will seek to derive a mantle magnitude M_m related to the seismic moment M_0 through

$$M_m = \log_{10} M_0 - 20 \tag{1}$$

where M_0 is in dyn-cm. We use the standard theory of excitation and propagation of surface waves to write the spectral amplitude of the transverse component of ground motion at distance Δ from the source:

$$X(\omega) = a\sqrt{\pi/2}[e^{-\omega a\Delta/2UQ}/\sqrt{\sin\Delta}] \cdot \left[\frac{1}{U}\,|l^{3/2}(lL_2p_L + iq_LL_1)|M_0\right] \tag{2}$$

where the notation follows the normal mode conventions of KANAMORI and STEWART (1976). In particular, L_1 and L_2 are the two excitation coefficients depending only on frequency and depth, and p_L and q_L trigonometric functions describing the relative orientation of the double-couple, the free surface, and the station; a is the radius of the earth and Δ is in radians. As in the case of Rayleigh waves, this equation expresses the separation of the propagation effects, regrouped in the first bracket, from the excitation terms, regrouped in the second bracket (HARKRIDER, 1964). Thus, the seismic moment (or equivalently the mantle magnitude) can still be retrieved from the spectral amplitude through

$$M_m = \log_{10} M_0 - 20 = \log_{10} X(\omega) + C_D + C_S + C_0. \tag{3}$$

In this equation, identical to Equation (5) of Paper I, the corrections C_D and C_S will take values different from their Rayleigh counterparts, reflecting the different excitation of Love waves, and in the case of C_D, the different values of the attenuation Q^{-1} and dispersion U. The "locking" constant remains $C_0 = \log_{10}(\sqrt{2/\pi}/a) = -0.90$ if $X(\omega)$ is measured in μm-s.

An additional problem is that the asymptotic summation of normal modes inherent in Equation (2) does not take into account the possible effect of overtones. This point was not discussed in Paper I since mantle Rayleigh overtones travel at

faster group velocities than the fundamental mode (typically 4.4 km/s for the first branch; see OKAL and JO (1983)), and we could assume that the fundamental had been effectively extracted from the record before processing, either visually, or through automatic group velocity windowing. Over oceanic paths, fundamental Love waves of 30–80 s period can be contaminated by overtones traveling at very similar group velocities (e.g., THATCHER and BRUNE, 1969; BOORE, 1969); the accurate study of their dispersion requires sophisticated filtering techniques (e.g., FORSYTH, 1975; CARA, 1978). Accordingly, in Section 4, we will study theoretically the possible influence of overtone contamination on measured values of M_m. We will show that the quality of the measurements is not expected to suffer significantly, a result confirmed by testing on a real dataset the effect of using a narrower range of frequencies ($T \geq 80$ s as opposed to $T \geq 50$ s). In anticipation of those results, we will at this point develop the theory for all periods $T \geq 50$ s, reserving a full discussion for Section 4.

Distance Correction C_D

The distance correction remains

$$C_D = \tfrac{1}{2} \log_{10} \sin \Delta + (\log_{10} e) \frac{\omega a \Delta}{2UQ} \tag{4}$$

where the values of U and Q used to correct for the effect of anelastic attenuation must be compiled from available models of Love wave attenuation. In order to reflect the possible effect of lateral heterogeneity, we keep the regionalized tectonic model used in Paper I (see Figure 1), and list in Table 1 values of Q and U

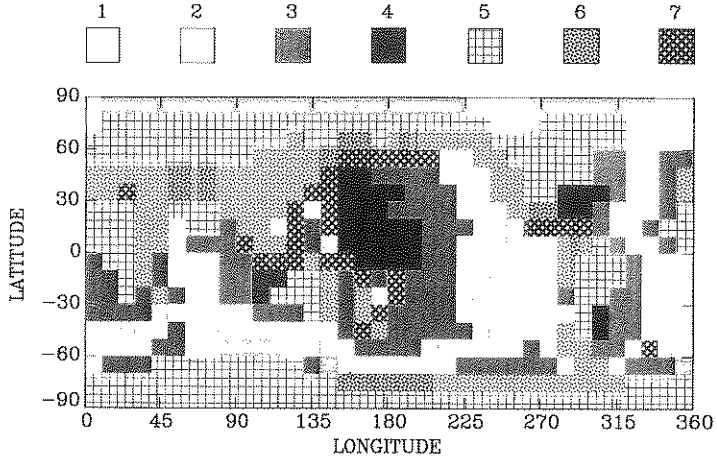

Figure 1

Tectonic regionalization used in the computation of the distance correction C_D. The various shading patterns refer to oceans (1: less than 20 Ma; 2: 20–50 Ma; 3: 50–100 Ma; 4: older than 100 Ma); continents (5: shields; 6: tectonic regions); and trenches (7). See Table 1 for corresponding values of U and Q.

Table 1

Regionalized Love Dispersion and Attenuation Models Used in Computing Distance Correction

	Region 1 0–20 Ma		Region 2 20–50 Ma		Region 3 50–100 Ma		Region 4 > 100 Ma		Region 5 Shields		Region 6 Mountains		Region 7 Trenches	
T, s	*U*, km/s	*Q*	*U*, km/s	*Q*	*U*, km/s	*Q*	*U*, km/s	*Q*	*U*, km/s	*Q*	*U*, km/s	*Q*	*U*, km/s	*Q*
50	4.15	135	4.31	133	4.39	144	4.44	160	3.78	244	3.77	140	3.80	115
60	4.15	132	4.31	133	4.39	144	4.44	161	3.93	223	3.93	126	4.01	107
70	4.16	130	4.31	132	4.38	145	4.44	161	4.04	212	4.04	118	4.09	100
80	4.16	129	4.30	132	4.38	144	4.43	162	4.12	204	4.12	115	4.12	94
90	4.16	128	4.30	132	4.38	144	4.43	163	4.18	200	4.19	113	4.16	95
111	4.17	127	4.30	132	4.37	145	4.42	164	4.26	192	4.25	112	4.19	99
127	4.17	128	4.30	133	4.37	146	4.42	167	4.29	188	4.28	114	4.22	102
145	4.17	129	4.29	135	4.36	147	4.41	169	4.32	187	4.32	117	4.26	105
167	4.18	131	4.29	137	4.36	149	4.41	171	4.34	185	4.34	120	4.29	108
193	4.18	133	4.29	140	4.36	151	4.40	175	4.36	183	4.36	123	4.32	112
223	4.19	136	4.30	143	4.35	155	4.40	179	4.39	183	4.38	128	4.36	116
259	4.20	143	4.31	149	4.36	158	4.40	183	4.41	183	4.41	132	4.39	125
300	4.22	149	4.33	155	4.38	160	4.42	188	4.45	185	4.45	140	4.42	133

compiled or computed from the works of KANAMORI (1970), CANAS and MITCHELL (1978), MITCHELL and YU (1980), NAKANISHI (1981) and HWANG and MITCHELL (1987). The computation of C_D proceeds exactly as in the case of Rayleigh waves: The path is split into segments belonging to the various provinces, and their contributions to the second term in C_D added.

Source Correction C_S

Just as for Rayleigh waves, this correction is approximated in order to ignore the focal mechanism and exact depth of the earthquake, which are assumed to be unknown at the time of the measurement.

We computed the expression of the excitation coefficients L_1 and L_2 of the earth's fundamental toroidal modes between periods of 40 and 300 s, using the PREM model (DZIEWONSKI and ANDERSON, 1981). As in Paper I, we define the source excitation E of a Love wave at angular frequency ω and in a particular geometry as

$$E(\phi_f, \delta, \lambda; \phi_s; h; \omega) = \frac{1}{U} \left| l^{3/2}(lL_2 p_L + iL_1 q_L) \right| \tag{5}$$

and L_{av}, the "logarithmic average excitability", as the logarithm of the average of E, taken over a large number (in practice 3240) of combinations of focal geometry and station azimuth. Figure 2a is a plot (similar to Figure 3a of Paper I) of the behavior of L_{av} with period and depth, in the period interval range 40–300 s. The sampling depths used are the same as in the Rayleigh study.

On this figure, it is immediately apparent that, in this range of depths, the excitation of Love waves is less sensitive to depth than that of Rayleigh waves. A

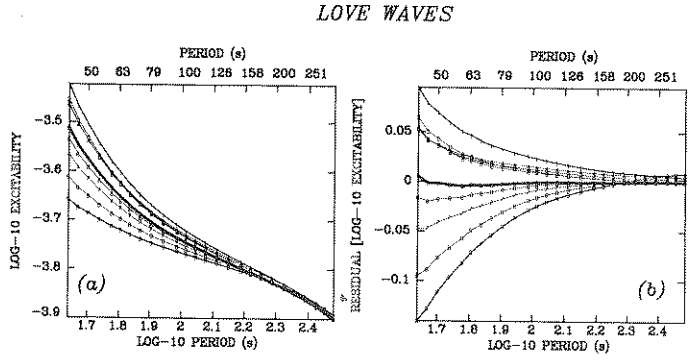

Figure 2

(a): Logarithmic average excitability for fundamental Love waves plotted as a function of period and depth. The various symbols (from 0 to 9) refer to ten sampling depths between 10 and 75 km. The thicker trace corresponds to $h = 25$ km, which is retained for the computation of C_S. (b): Same as left, after the correction C_S given by (7) has been applied.

simple explanation for this situation stems from the different behavior of the two waves' eigenfunctions: Elementary Love and Rayleigh theory shows that in a layer of velocities α and β, the vertical gradients of the potentials are on the other order of

$$\frac{1}{\Phi}\frac{\partial \Phi}{\partial z} = k_x \left| \frac{c^2}{\alpha^2} - 1 \right|^{1/2} \tag{6a}$$

and

$$\frac{1}{\Psi}\frac{\partial \Psi}{\partial z} = k_x \left| \frac{c^2}{\beta^2} - 1 \right|^{1/2} \tag{6b}$$

where k_x is the horizontal wavenumber. For both kinds of waves, the phase velocity c at the periods we are considering is close to the shear wave velocities in the lid or upper mantle (all are typically in the 4 to 5 km/s range), and the corresponding shear potentials Ψ show little variation with depth. Rayleigh waves alone feature the compressional potential Φ, for which c/α is significantly different from 1, resulting in strong variations of eigenfunctions, and hence of excitation coefficients, with depth.

Next, we eliminate true focal depth altogether by selecting the intermediate value 25 km, modeling L_{av} as a cubic spline, and retaining $C_s = -L_{av}$ as the source correction to be used in (3); the result is

$$C_S = 0.80263\,\theta^3 + 0.13524\,\theta^2 + 0.28570\,\theta + 3.8112 \tag{7}$$

where $\theta = \log_{10} T - 2.2354$, with the period T in seconds. Figure 2b confirms that the systematic error introduced by neglecting true depth and using (7) is extremely small for Love waves, ranging from -0.05 to 0.04 units of magnitude for $T \geq 80$ s, and not exceeding 0.12 units at $T = 50$ s. In particular, this source of error becomes totally negligible at the lower-frequency end of the spectrum, where hopefully most of our measurements will be taken.

Impossibility of Time-domain Measurements

In the case of mantle Rayleigh waves, we were able to relate the spectral amplitude $X(\omega)$ involved in the definition of M_m directly to the amplitudes A observed in the time-domain oscillation of the seismogram, and thus to propose a time-domain measurement M_m^{TD} of the mantle magnitude. This was because the fundamental branch of Rayleigh is strongly (and actually, inversely) dispersed in the corresponding range of frequencies (Paper I and OKAL, 1989). In the case of Love waves, this dispersion is absent from most oceanic structures and only very weak in continental ones (see Table 1); therefore it is not possible to develop a time-domain mantle magnitude similar to M_m^{TD} for Love waves.

3. Application to Data

Having obtained theoretical expressions for C_D and C_S in (3), we now apply the concept of the mantle magnitude M_m to a real-life dataset of long-period teleseismic Love waves, and to analyze the results critically, in parallel to the discussion of the Rayleigh wave M_m in Paper I.

We targeted for this study all GEOSCOPE records (from 1982 to February, 1987) for shallow events ($h \leq 75$ km), with reported seismic moments larger than 10^{26} dyn-cm. After extraction of the horizontal components, a visual check was made of each record, at which time those featuring instrumental instability were eliminated. We also did not consider records from station MBO (M'Bour, Sénégal), for which absolute gains are in doubt. A total of 271 GEOSCOPE records were used, corresponding to 1st or 2nd passages G_1 or G_2. In addition, and in order to test the performance of the distance correction C_D, we repeated our experiment in Paper I for Rayleigh waves by targeting higher passages (up to and including G_5) of the 1986 Aleutian event. The 26 additional records are treated separately in the discussion, and are not included in the statistical analysis.

An additional dataset consists of 36 1st passages G_1 recorded at Papeete, Tahiti (PPT), on the LDG broad-band instruments of the Polynesian network. On the other hand, we did not use any records from the long-period instruments at Pasadena, for lack of a system offering characteristics of instrumental stability and continuity of recording over large periods of time comparable to the Vertical ULP33 used in Paper I. The total dataset thus includes 333 records, from 85 earthquakes. Published estimates of seismic moments, as well as focal geometry parameters were taken from the Harvard Centroid Moment Tensor solutions (DZIEWONSKI *et al.*, 1983a–c, 1984a–c, 1985a–d, 1986a–c, 1987a–e, 1988a–d, 1989), and are listed in Table 2. Figures 3 and 4 plot the epicenters and mechanisms of all the events used in this study.

Typical examples of the signals used are given in Figure 5; instrumental characteristics and responses are discussed in Paper I and ROMANOWICZ *et al.* (1984). After visual inspection, data processing involved isolation of the Love wave through time-windowing, Fourier-transforming of each of the 666 horizontal components, instruments deconvolution, and rotation into natural Love polarization. At each of the Fourier periods, Equations (3) and (7) were used to compute an estimate of the mantle magnitude, and the largest value retained as M_m. These values were then compared to the value $M_m^{\text{pub}} = \log_{10} M_0 - 20$ equivalent to the published value M_0 of the seismic moment, and the residual $r = M_m - M_m^{\text{pub}}$ defined.

As in the case of Rayleigh waves in Paper I, the resulting dataset is listed in its entirety in Tables 3 and 4, and Figure 6 plots the computed values of M_m against the published values of the seismic moment M_0.

Table 2

Source Parameters of Events Used in This Study

Date	Epicenter °N	Epicenter °E	Depth, km	Published Moment, 10^{27} dyn-cm	Focal Mechanism ϕ, deg	Focal Mechanism δ, deg	Focal Mechanism λ, deg	Reference
1979 02 28	60.64	-141.59	19	1.88	271	13	96	a
1979 03 14	17.81	-101.28	27	1.72	306	15	110	a
1981 07 06	-22.26	171.73	58	2.59	345	30	181	b
1981 09 01	-14.99	-173.17	20	1.94	115	37	287	b
1981 10 25	18.01	-102.11	32	0.70	287	20	82	b
1982 05 07	-60.68	-20.83	10	0.35	268	53	0	c
1982 06 07	16.62	-98.15	11	0.29	268	10	48	c
1982 07 23	36.21	141.76	27	0.39	203	14	86	c
1982 08 05	-12.70	165.94	24	0.32	337	32	83	c
1982 11 19	-10.59	-74.75	10	0.11	0	34	116	c
1982 12 19	-24.19	-175.77	29	1.98	198	22	101	c
1983 01 17	38.09	20.19	10	0.23	34	14	153	d
1983 01 24	16.18	-95.15	36	0.21	110	54	215	d
1983 03 18	-4.86	153.51	70	4.63	170	49	120	d
1983 04 03	8.73	-83.12	28	1.82	310	25	110	e
1983 05 26	40.37	139.15	13	4.55	16	27	86	e
1983 06 21	41.32	139.14	17	0.19	23	43	94	e
1983 07 11	-60.90	-52.94	14	0.33	0	60	205	f
1983 08 06	40.18	24.73	10	0.12	229	81	186	f
1983 08 17	55.79	161.21	77	0.41	216	41	60	f
1983 10 04	-26.62	-70.77	39	3.38	9	20	110	g
1983 10 22	-60.62	-25.44	10	0.46	231	35	278	g
1983 10 28	44.05	-113.89	14	0.31	304	29	257	g
1983 11 16	19.43	-155.45	11	0.11	130	25	5	g
1983 11 22	0.42	-79.94	35	0.17	33	24	133	g
1983 11 30	-6.89	72.12	10	4.05	293	35	308	g
1983 12 02	14.05	-91.94	31	0.37	296	19	89	g
1984 02 07	-9.92	160.46	22	2.52	296	37	30	h
1984 03 19	40.29	63.33	15	0.35	218	21	86	h
1984 03 24	44.16	148.29	31	0.64	229	17	109	h
1984 05 17	-36.46	53.54	10	0.25	1	64	177	i
1984 05 26	-43.83	39.14	10	0.13	98	88	0	i
1984 06 24	17.99	-69.35	16	0.14	352	6	155	i
1984 08 06	32.34	131.94	29	0.29	203	85	275	j
1984 09 18	33.97	141.44	35	0.21	264	26	220	j
1984 11 01	8.15	-38.76	10	0.40	274	73	183	k
1984 11 17	0.19	98.04	25	0.58	334	10	116	k
1984 11 23	-14.30	171.28	27	0.19	300	66	353	k
1984 12 28	56.17	163.58	22	0.14	260	61	162	k
1984 12 30	-36.73	177.50	19	0.18	86	56	348	k
1985 01 21	-1.01	128.53	21	0.14	203	76	188	l
1985 03 02	-1.98	119.70	44	0.12	283	84	357	l
1985 03 03	-33.15	-71.98	41	10.31	11	26	110	l
1985 04 09	-34.17	-71.54	47	0.50	0	21	99	m
1985 04 13	1.66	126.57	40	0.28	12	34	69	m
1985 05 10	-5.58	151.08	25	0.69	193	67	194	m
1985 07 03	-4.46	152.82	31	0.83	169	37	106	n
1985 07 22	-6.28	148.73	36	0.21	266	25	77	n
1985 08 23	39.42	75.27	15	0.33	315	29	159	n
1985 09 19	18.18	-102.57	21	10.99	301	18	105	n
1985 09 21	17.82	-101.67	21	2.49	296	17	85	n
1985 09 26	-34.63	-178.69	61	0.24	196	54	39	n
1985 11 17	-1.59	135.01	13	0.50	179	64	174	o
1985 11 28 A	-14.01	166.24	24	0.30	161	36	251	o
1985 11 28 B	-13.96	166.17	44	0.36	262	68	13	o
1985 12 21	-14.04	166.51	46	0.57	165	44	88	o

Table 2 (continued)

Source Parameters of Events Used in This Study

Date	Epicenter °N	Epicenter °E	Depth, km	Published Moment, 10^{27} dyn-cm	Focal Mechanism ϕ, deg	Focal Mechanism δ, deg	Focal Mechanism λ, deg	Reference
1985 12 23	62.21	-124.30	15	0.15	354	45	98	o
1986 03 24	-2.48	138.71	15	0.11	94	39	356	p
1986 04 20	-2.38	139.32	21	0.16	88	29	20	q
1986 04 30	18.41	-102.98	21	0.31	290	18	87	q
1986 05 07	51.41	-174.83	31	10.36	246	22	85	q
1986 07 09	1.96	126.59	35	0.16	9	39	71	r
1986 08 14	1.82	126.64	20	2.26	347	16	34	r
1986 10 14	-4.99	153.58	54	0.15	134	40	80	s
1986 10 20	-28.10	-176.43	50	4.52	270	56	158	s
1986 10 23	-10.98	165.17	15	0.14	332	15	97	s
1986 11 14	23.96	121.82	33	1.30	210	33	87	s
1987 01 03	-14.99	167.92	17	0.12	158	32	74	t
1987 01 05	52.46	-169.35	34	0.15	246	26	95	t
1987 01 30	-60.15	-26.83	15	0.33	232	16	123	t
1987 02 06	36.93	141.70	41	0.13	209	25	99	t
1987 02 08	-5.94	147.79	15	1.11	82	83	4	t
1987 02 13	0.69	126.24	37	0.14	18	42	83	t
1987 03 05	-24.49	-70.17	42	2.48	12	23	106	t
1987 03 06	0.15	-77.83	15	0.64	195	27	98	t
1987 06 27	-2.19	138.24	27	0.08	118	53	5	u
1987 07 06	-27.02	-108.25	15	0.15	249	44	293	v
1987 08 08	-19.19	-70.14	80	0.79	176	20	273	v
1987 09 03	-58.90	158.30	15	1.38	155	69	188	v
1987 10 06	-17.90	-172.29	15	0.89	352	42	247	w
1987 10 12	-7.29	154.39	18	0.34	323	43	292	w
1987 10 16	-6.25	149.09	48	1.26	266	32	90	w
1987 10 25	-2.39	138.41	15	0.19	22	32	132	w
1987 11 27	-16.37	168.10	15	0.02	151	69	3	w
1987 11 30	58.68	-142.79	15	7.27	355	70	188	w

References: a: Dziewonski *et al.* (1987*a*); b: Dziewonski *et al.* (1988*a*); c: Dziewonski *et al.* (1983*a*); d: Dziewonski *et al.* (1983*b*); e: Dziewonski *et al.* (1983*c*); f: Dziewonski *et al.* (1984*a*); g: Dziewonski *et al.* (1984*b*); h: Dziewonski *et al.* (1984*c*); i: Dziewonski *et al.* (1985*a*); j: Dziewonski *et al.* (1985*b*); k: Dziewonski *et al.* (1985*c*); l: Dziewonski *et al.* (1985*d*); m: Dziewonski *et al.* (1986*a*); n: Dziewonski *et al.* (1986*b*); o: Dziewonski *et al.* (1986*c*); p: Dziewonski *et al.* (1987*b*); q: Dziewonski *et al.* (1987*c*); r: Dziewonski *et al.* (1987*d*); s: Dziewonski *et al.* (1987*e*); t: Dziewonski *et al.* (1988*b*); u: Dziewonski *et al.* (1988*c*); v: Dziewonski *et al.* (1988*d*); w: Dziewonski *et al.* (1989).

4. Discussion

Accuracy of M_m: The Population of Residuals r

It is immediately apparent that the residuals r are somewhat more scattered than in the case of Rayleigh waves (see Figure 8 of Paper I). While the average $\bar{r}$ and standard deviation σ of the residuals are comparable at the GEOSCOPE stations ($\bar{r} = 0.15$; $\sigma = 0.26$ for Love waves; $\bar{r} = 0.18$; $\sigma = 0.24$ for Rayleigh waves), values of M_m at Papeete are significantly deficient ($\bar{r} = -0.13$) and above all greatly scattered ($\sigma = 0.34$). Comparable numbers for Rayleigh waves at PPT were $\bar{r} = 0.09$; $\sigma =$

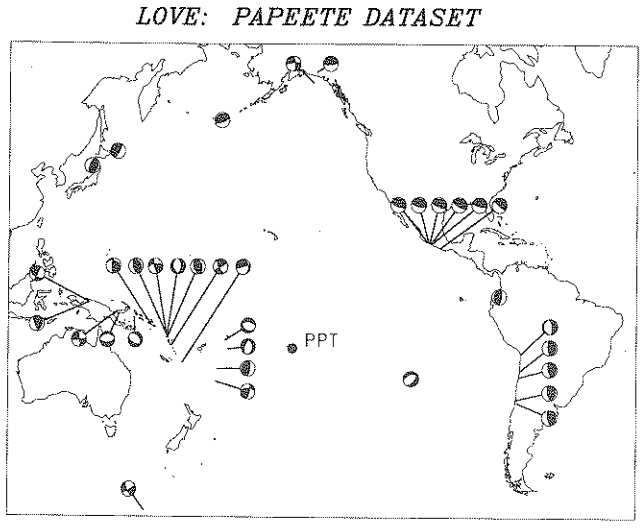

Figure 3
Map of epicenters and focal mechanisms for the Papeete dataset.

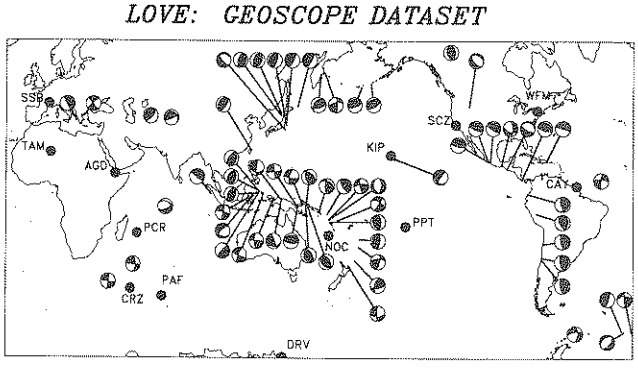

Figure 4
Map of epicenters and focal mechanisms for the GEOSCOPE dataset. Individual stations are shown as dots; the post-1986 location of the Réunion station at RER, only 18 km from PCR, is not shown.

0.19. In a later section, we will show that this is largely due to a focal machanism effect resulting from the particular geometry of the station PPT with respect to the major subduction zones.

Taken as a whole, the dataset features an average residual $\bar{r} = 0.12$, with a standard deviation $\sigma = 0.29$ units of magnitude (Table 5). These numbers compare reasonably with their Rayleigh counterparts, and indicate that Love waves can indeed be used to obtain a real-time one-station estimate of the moment of a teleseismic event.

Table 3
Papeete Dataset

Event	Station	Passage	Δ	M_m^{pub}	M_m	T	r	M_c	r_c
1979 02 28	PPT	1	78.34	7.27	6.48	82	-0.79	7.08	-0.19
1979 03 14	PPT	1	59.17	7.24	7.12	102	-0.12	7.27	0.03
1981 07 06	PPT	1	36.59	7.41	7.70	137	0.29	7.57	0.16
1981 07 15	PPT	1	40.79	6.76	6.72	102	-0.04	6.73	-0.03
1981 09 01	PPT	1	22.72	7.29	7.58	82	0.29	8.10	0.81
1981 10 25	PPT	1	58.68	6.85	6.74	68	-0.11	6.78	-0.07
1982 06 07 A	PPT	1	61.04	6.46	6.24	82	-0.22	6.49	0.03
1982 06 07 B	PPT	1	60.84	6.43	6.26	102	-0.17	6.46	0.03
1982 08 05	PPT	1	43.16	6.51	6.48	82	-0.03	6.38	-0.13
1982 12 19	PPT	1	25.39	7.30	7.26	137	-0.04	7.44	0.14
1983 05 26	PPT	1	87.84	7.66	7.36	102	-0.30	7.87	0.21
1983 10 04	PPT	1	72.74	7.53	7.00	82	-0.53	7.48	-0.05
1984 02 07	PPT	1	48.97	7.40	7.63	205	0.23	7.36	-0.04
1984 03 24	PPT	1	83.67	6.80	6.62	68	-0.18	7.29	0.49
1985 03 03	PPT	1	70.32	8.01	7.73	137	-0.28	8.16	0.15
1985 04 09	PPT	1	70.53	6.70	6.06	68	-0.64	6.96	0.26
1985 09 19	PPT	1	58.40	8.04	7.71	137	-0.33	7.77	-0.27
1985 09 21	PPT	1	58.87	7.40	7.21	102	-0.19	7.34	-0.06
1985 11 28 A	PPT	1	42.58	6.48	6.66	82	0.18	6.70	0.22
1985 11 28 B	PPT	1	42.64	6.56	6.76	82	0.20	6.46	-0.10
1985 12 21	PPT	1	42.33	6.76	6.77	59	0.01	6.78	0.02
1986 04 30	PPT	1	58.18	6.49	6.36	82	-0.13	6.42	-0.07
1986 05 07	PPT	1	72.38	8.02	6.93	137	-1.09	7.73	-0.29
1986 10 20	PPT	1	27.08	7.95	7.83	102	-0.12	7.62	-0.33
1987 02 08	PPT	1	62.16	7.05	7.60	102	0.55	7.29	0.24
1987 03 05	PPT	1	73.50	7.39	6.64	82	-0.75	6.89	-0.50
1987 03 06	PPT	1	75.33	6.80	6.55	82	-0.25	7.04	0.24
1987 06 27	PPT	1	72.44	5.92	6.08	51	0.16	5.73	-0.19
1987 07 06	PPT	1	41.06	5.98	6.22	82	0.24	6.10	0.12
1987 08 08	PPT	1	74.88	6.90	6.44	59	-0.46	7.09	0.19
1987 09 03	PPT	1	55.90	7.15	7.22	82	0.07	6.75	-0.40
1987 10 06	PPT	1	21.63	6.95	6.63	51	-0.32	7.15	0.20
1987 10 12	PPT	1	55.49	6.53	6.38	102	-0.15	6.31	-0.22
1987 10 16	PPT	1	60.83	7.11	7.12	102	0.01	7.08	-0.03
1987 25 10	PPT	1	72.15	6.28	6.50	51	0.22	6.49	0.21
1987 11 30	PPT	1	76.31	7.86	8.04	205	0.18	7.61	-0.25

Slope of $\log_{10} M_0$ *vs.* M_m

In developing a variable-period mantle magnitude, one of our primary goals was to avoid the saturation effects known to affect traditional magnitude scales involving measurements at a fixed period (GELLER, 1976). In this respect, the behavior of M_m for events with very large moments is of crucial importance; our theory predicts that M_m should keep growing as $\log_{10} M_0$. In order to test this behavior, we regressed $\log_{10} M_0$ as a function of M_m, for each of the datasets in Figure 6. The best-fitting slope is 0.99 for the GEOSCOPE dataset, but only 0.83 for the PPT dataset. Again, we take the latter as reflecting an artifact of focal geometries. For the whole dataset, the best-fitting slope is 0.96, not significantly different from 1, and indicating that the Love wave mantle magnitude M_m successfully avoids saturation at higher magnitudes.

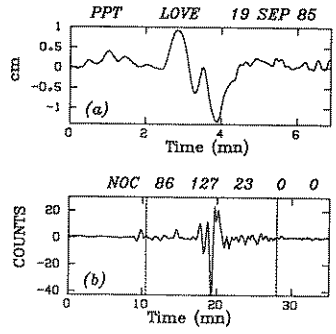

Figure 5
Typical examples of records used in this study. In both instances, the individual horizontal components have been rotated to *SH* polarization. (a): PPT record of the 19 September 1985 Mexican earthquake. (b): Record of the 07 May 1986 Aleutian event at the GEOSCOPE station NOC (Nouméa, New Caledonia). The first passage G_1 is shown, with the time window actually used in the determination of M_m outlined by the dotted lines.

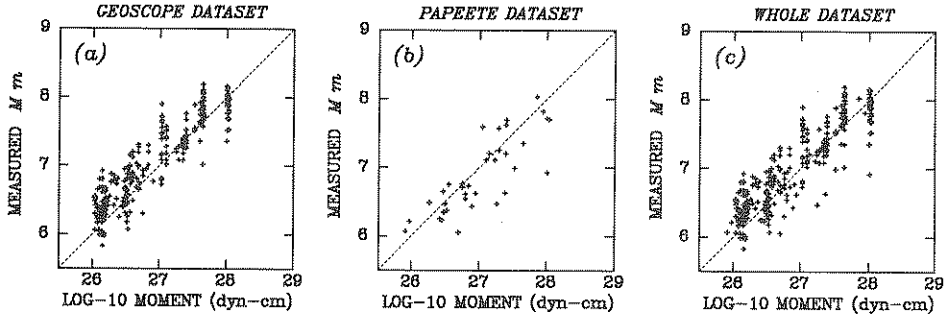

Figure 6
Measured values of M_m plotted as a function of the published seismic moment M_0, either for individual datasets (a, b), or the whole dataset (c). The dashed line is the theoretical relation $M_m = \log_{10} M_0 - 20$.

Influence of Focal Mechanism and True Depth

In using (7) as a source correction, and in keeping with the magnitude concept, we ignore the true focal parameters of the earthquake, and introduce a systematic error in the estimate of its seismic moment. In order to investigate the extent of this error, and its contribution to r, we used, for each record, the published centroid moment tensor to compute the true value of the excitation E given by (5), and obtain a "focal mechanism contribution"

$$C_{FM} = \log_{10} E - C_S \tag{8}$$

and a corrected value of M_m

$$M_c = M_m + C_{FM}. \tag{9}$$

Table 4

GEOSCOPE Dataset

Event	Station	Passage	Δ	M_m^{pub}	M_m	T	r	M_c	r_c
1982 05 07	SSB	1	107.77	6.54	6.96	256	0.42	6.67	0.13
1982 07 23	SSB	1	89.99	6.59	6.77	64	0.18	6.92	0.33
1982 11 19	SSB	1	90.05	6.04	6.31	128	0.27	6.18	0.14
1982 12 19	PCR	1	112.60	7.30	7.29	160	-0.01	7.25	-0.05
1982 12 19	PCR	2	247.40	7.30	7.09	85	-0.21	7.05	-0.25
1983 01 17	SSB	1	13.71	6.36	6.74	64	0.38	6.82	0.46
1983 01 17	PCR	1	67.84	6.36	6.52	128	0.16	6.62	0.26
1983 01 24	PCR	1	151.86	6.32	6.79	64	0.47	6.48	0.16
1983 03 18	PCR	1	95.61	7.66	7.67	160	0.01	7.93	0.27
1983 03 18	PCR	2	264.39	7.66	7.67	85	0.01	7.96	0.30
1983 03 18	SSB	1	131.44	7.66	7.70	71	0.04	8.77	1.11
1983 04 03	PCR	1	138.35	7.26	7.26	256	0.00	7.73	0.47
1983 04 03	PCR	2	221.65	7.26	7.26	75	0.00	7.66	0.40
1983 04 03	SSB	1	82.18	7.26	7.21	213	-0.05	7.38	0.12
1983 05 26	PAF	1	108.11	7.66	7.73	183	0.07	7.77	0.11
1983 05 26	PAF	2	251.89	7.66	7.96	142	0.30	8.00	0.34
1983 05 26	PCR	1	98.82	7.66	7.78	183	0.12	7.67	0.01
1983 05 26	PCR	2	261.18	7.66	7.75	256	0.09	7.64	-0.02
1983 05 26	SSB	2	274.63	7.66	7.73	213	0.07	7.62	-0.04
1983 06 21	SSB	1	84.54	6.28	6.89	116	0.61	6.69	0.41
1983 07 11	PAF	1	60.83	6.52	6.89	183	0.37	6.84	0.32
1983 07 11	SSB	1	115.75	6.52	6.19	213	-0.33	6.75	0.23
1983 08 06	SSB	1	15.67	6.08	6.66	64	0.58	6.31	0.23
1983 08 17	PCR	1	116.07	6.61	6.87	183	0.26	6.67	0.06
1983 08 17	SSB	1	77.22	6.61	6.50	116	-0.11	6.51	-0.10
1983 10 04	PAF	1	96.61	7.53	7.55	213	0.02	7.66	0.13
1983 10 04	PCR	1	109.48	7.53	7.52	213	-0.01	7.51	-0.02
1983 10 04	PCR	2	250.52	7.53	7.90	80	0.37	7.91	0.38
1983 10 04	SSB	1	99.03	7.53	7.56	71	0.03	7.57	0.04
1983 10 22	PAF	1	51.10	6.66	6.69	128	0.03	6.87	0.21
1983 10 22	PCR	1	67.32	6.66	7.04	160	0.38	6.86	0.20
1983 10 22	SSB	1	108.50	6.66	6.82	142	0.16	6.76	0.10
1983 10 28	PCR	1	155.57	6.49	6.69	85	0.20	6.79	0.30
1983 11 16	PAF	1	132.97	6.03	6.54	213	0.51	6.40	0.37
1983 11 16	SSB	1	112.92	6.04	6.07	142	0.03	6.08	0.04
1983 11 22	PAF	1	124.86	6.23	6.43	91	0.20	6.37	0.14
1983 11 22	SSB	1	85.80	6.23	6.43	116	0.20	6.37	0.14
1983 11 22	TAM	1	85.65	6.23	6.49	107	0.26	6.45	0.22
1983 11 30	PAF	1	42.42	7.61	7.37	91	-0.24	8.23	0.62
1983 11 30	PAF	2	317.58	7.61	7.63	95	0.02	8.50	0.89
1983 11 30	PCR	1	21.43	7.61	7.82	256	0.21	7.60	-0.01
1983 11 30	PCR	2	338.57	7.61	7.83	151	0.22	7.61	0.00
1983 11 30	SSB	1	79.52	7.61	7.93	107	0.32	7.71	0.10
1983 11 30	SSB	2	280.48	7.61	7.62	256	0.01	7.41	-0.20
1983 11 30	TAM	1	71.49	7.61	7.76	80	0.15	7.66	0.05
1983 11 30	TAM	2	288.51	7.61	7.66	256	0.05	7.55	-0.06
1983 12 02	PAF	1	141.83	6.57	6.74	98	0.17	6.75	0.18
1983 12 02	SSB	1	84.56	6.57	6.33	213	-0.24	6.56	-0.01
1983 12 02	TAM	1	91.30	6.57	6.74	256	0.17	6.75	0.18
1984 02 07	PCR	1	100.02	7.40	7.34	116	-0.06	7.63	0.23
1984 02 07	SSB	1	139.10	7.40	7.35	67	-0.05	7.69	0.29
1984 02 07	SSB	2	220.90	7.40	7.45	284	0.05	7.95	0.55
1984 02 07	TAM	1	152.80	7.40	7.77	98	0.37	7.60	0.20
1984 02 07	TAM	2	207.20	7.40	7.68	171	0.28	7.50	0.10
1984 03 19	SSB	1	42.55	6.54	6.08	213	-0.46	6.39	-0.15
1984 03 19	TAM	1	51.34	6.54	6.57	75	0.03	6.54	0.00
1984 03 24	TAM	1	105.02	6.81	6.96	64	0.15	7.29	0.48
1984 05 17	TAM	1	74.47	6.40	6.26	213	-0.14	6.91	0.51
1984 05 26	TAM	1	73.26	6.11	6.00	80	-0.11	6.29	0.18

Table 4

GEOSCOPE Dataset

Event	Station	Passage	Δ	M_m^{pub}	M_m	T	r	M_c	r_c
1984 05 26	WFM	1	132.90	6.11	6.69	128	0.58	6.24	0.13
1984 05 26	WFM	2	227.10	6.11	6.81	102	0.70	6.36	0.25
1984 06 24	WFM	1	24.97	6.15	6.05	64	-0.10	6.49	0.34
1984 08 06	SSB	1	88.95	6.46	6.40	213	-0.06	6.82	0.36
1984 08 06	TAM	1	104.77	6.46	6.49	71	0.03	6.91	0.45
1984 09 18	WFM	1	96.82	6.32	6.43	67	0.11	6.98	0.66
1984 11 01	PCR	1	96.94	6.60	7.21	80	0.61	6.80	0.20
1984 11 01	SSB	1	52.54	6.60	6.83	256	0.23	6.78	0.18
1984 11 01	TAM	1	44.90	6.60	7.13	85	0.53	6.88	0.28
1984 11 01	WFM	1	46.54	6.60	6.91	64	0.31	7.18	0.58
1984 11 17	PCR	1	46.61	6.76	6.31	80	-0.45	7.22	0.46
1984 11 17	SSB	1	92.35	6.76	6.94	75	0.18	7.35	0.59
1984 11 17	WFM	1	136.77	6.76	6.86	85	0.10	7.13	0.37
1984 11 23	WFM	1	117.36	6.28	6.77	256	0.49	6.39	0.11
1984 11 23	WFM	2	242.64	6.28	6.76	135	0.48	6.40	0.12
1984 12 28	SSB	1	77.21	6.15	6.81	91	0.66	6.40	0.25
1984 12 28	WFM	1	69.93	6.15	6.00	71	-0.15	6.65	0.50
1984 12 30	WFM	1	125.88	6.26	6.56	98	0.30	6.43	0.17
1985 01 21	TAM	1	120.61	6.15	6.82	98	0.67	6.34	0.19
1985 01 21	WFM	1	133.64	6.15	6.93	67	0.78	6.46	0.31
1985 01 21	WFM	2	226.36	6.15	6.69	142	0.54	6.21	0.06
1985 03 02	SSB	1	108.91	6.04	6.49	80	0.45	6.46	0.42
1985 03 02	TAM	1	113.01	6.04	6.56	183	0.52	6.09	0.05
1985 03 03	PAF	1	91.08	8.01	8.03	142	0.02	8.06	0.05
1985 03 03	PAF	2	268.92	8.01	8.06	78	0.05	8.10	0.09
1985 03 03	SSB	1	104.42	8.01	8.11	128	-0.10	8.01	0.00
1985 03 03	SSB	2	255.58	8.01	8.17	142	0.16	8.07	0.06
1985 03 03	TAM	1	68.94	8.01	7.93	256	-0.08	8.11	0.10
1985 03 03	WFM	1	14.24	8.01	7.37	91	-0.64	7.77	-0.24
1985 03 03	WFM	2	345.76	8.01	7.99	91	-0.02	8.39	0.38
1985 04 09	PCR	1	105.32	6.70	6.67	213	-0.03	6.64	-0.06
1985 04 09	TAM	1	92.60	6.70	6.66	160	-0.04	6.82	0.12
1985 04 09	WFM	1	76.64	6.70	6.76	91	0.06	7.30	0.60
1985 04 13	TAM	1	117.67	6.45	6.42	107	-0.03	7.28	0.83
1985 05 10	TAM	1	142.61	6.84	7.31	80	0.47	6.98	0.14
1985 05 10	PCR	1	93.10	6.84	7.02	160	0.18	6.91	0.07
1985 05 10	WFM	1	125.39	6.84	7.21	64	0.37	7.07	0.23
1985 07 03	PCR	1	95.12	6.92	6.78	71	-0.14	7.87	0.95
1985 07 22	SSB	1	130.22	6.32	6.86	71	0.54	6.81	0.49
1985 08 23	AGD	1	40.01	6.52	6.98	85	0.46	6.79	0.27
1985 08 23	CAY	1	114.56	6.52	6.82	64	0.30	6.81	0.29
1985 09 19	AGD	1	134.79	8.04	7.98	160	-0.06	8.08	0.04
1985 09 19	AGD	2	225.21	8.04	7.82	160	-0.22	7.92	-0.12
1985 09 19	CAY	1	50.79	8.04	8.00	67	-0.04	8.17	0.13
1985 09 19	CAY	2	309.21	8.04	7.79	151	-0.25	8.06	0.02
1985 09 19	PCR	1	159.22	8.04	8.00	80	-0.04	8.25	0.21
1985 09 19	PCR	2	200.78	8.04	7.69	142	-0.35	8.02	-0.02
1985 09 19	SSB	1	88.64	8.04	7.90	85	-0.14	8.11	0.07
1985 09 19	SSB	2	271.36	8.04	7.54	183	-0.50	7.76	-0.28
1985 09 21	AGD	1	134.34	7.40	7.39	64	-0.01	7.56	0.16
1985 09 21	AGD	2	225.66	7.40	7.26	160	-0.14	7.43	0.03
1985 09 21	CAY	1	49.89	7.40	7.35	256	-0.05	7.57	0.17
1985 09 21	CAY	2	310.11	7.40	7.53	75	0.13	7.69	0.29
1985 09 21	PCR	1	158.31	7.40	7.46	75	0.06	7.65	0.25
1985 09 21	PCR	2	201.69	7.40	7.36	75	-0.04	7.56	0.16
1985 09 21	SSB	1	88.32	7.40	7.29	80	-0.11	7.67	0.27
1985 09 26	CAY	1	122.37	6.38	6.82	91	0.44	6.57	0.19
1985 11 17	AGD	1	92.46	6.69	7.28	183	0.59	6.86	0.17
1985 11 17	AGD	2	267.54	6.69	7.32	107	0.63	6.90	0.21
1985 11 17	PCR	1	79.57	6.69	7.01	64	0.32	6.68	-0.01
1985 11 17	SSB	1	118.50	6.69	6.99	107	0.30	7.15	0.46

Table 4
GEOSCOPE Dataset

Event	Station	Passage	Δ	M_m^{pub}	M_m	T	r	M_c	r_c
1985 11 17	TAM	1	126.66	6.69	7.20	71	0.51	6.97	0.28
1985 11 28 A	AGD	1	124.88	6.48	6.67	64	0.19	6.89	0.41
1985 11 28 A	AGD	2	235.12	6.48	6.54	91	0.06	6.75	0.27
1985 11 28 A	CAY	1	140.97	6.48	6.78	91	0.30	6.84	0.36
1985 11 28 A	TAM	1	159.74	6.48	6.96	116	0.48	6.79	0.31
1985 11 28 B	AGD	1	124.81	6.56	7.16	256	0.60	6.76	0.20
1985 11 28 B	AGD	2	235.19	6.56	7.00	142	0.44	6.60	0.04
1985 11 28 B	CAY	1	141.04	6.56	7.01	91	0.45	6.69	0.13
1985 11 28 B	CAY	2	218.96	6.56	6.82	98	0.26	6.49	-0.07
1985 11 28 B	PCR	1	103.40	6.56	6.88	107	0.32	6.50	-0.06
1985 11 28 B	TAM	1	159.66	6.56	6.82	71	0.26	7.04	0.48
1985 11 28 B	TAM	2	200.34	6.56	6.83	213	0.27	7.01	0.45
1985 12 23	CAY	1	77.29	6.18	6.29	160	0.11	6.20	0.02
1985 12 23	SSB	1	65.13	6.18	6.68	256	0.50	6.47	0.29
1985 12 23	WFM	1	34.94	6.18	6.27	64	0.09	6.22	0.04
1986 03 24	AGD	1	96.26	6.05	6.52	107	0.47	6.22	0.17
1986 03 24	NOC	1	33.18	6.05	6.54	256	0.49	6.62	0.57
1986 03 24	WFM	1	130.19	6.05	6.43	80	0.38	6.34	0.29
1986 04 20	CAY	1	168.11	6.20	6.54	91	0.34	6.36	0.16
1986 04 20	NOC	1	32.77	6.20	6.29	213	0.09	6.79	0.59
1986 04 20	SSB	1	121.71	6.20	6.36	128	0.16	6.35	0.15
1986 04 30	AGD	1	134.95	6.49	6.54	160	0.05	6.63	0.14
1986 04 30	CAY	1	51.21	6.49	6.50	71	0.01	6.72	0.23
1986 04 30	KIP	1	51.60	6.49	6.32	71	-0.17	6.60	0.11
1986 04 30	NOC	1	97.48	6.49	6.65	91	0.16	6.67	0.18
1986 04 30	WFM	1	34.14	6.49	6.44	64	-0.05	6.71	0.22
1986 05 07	AGD	1	109.23	8.02	7.94	98	-0.08	8.13	0.11
1986 05 07	AGD	2	250.77	8.02	7.90	284	-0.12	8.09	0.07
1986 05 07	CAY	1	105.52	8.02	7.78	213	-0.24	8.24	0.22
1986 05 07	CAY	2	254.48	8.02	7.91	85	-0.11	8.30	0.28
1986 05 07	DRV	1	122.77	8.02	8.06	183	0.04	8.01	-0.01
1986 05 07	DRV	2	237.23	8.02	7.98	213	-0.04	7.93	-0.09
1986 05 07	KIP	1	32.70	8.02	7.70	256	-0.32	8.18	0.16
1986 05 07	KIP	2	327.30	8.02	7.53	75	-0.49	8.02	0.00
1986 05 07	NOC	1	75.28	8.02	8.15	183	0.13	8.11	0.09
1986 05 07	NOC	2	284.72	8.02	8.03	256	0.01	7.99	-0.03
1986 05 07	PAF	1	139.78	8.02	8.04	67	0.02	8.53	0.51
1986 05 07	PAF	2	220.22	8.02	7.71	183	-0.31	8.44	0.42
1986 05 07	SSB	1	83.50	8.02	7.98	256	-0.04	8.09	0.07
1986 05 07	SSB	2	276.50	8.02	7.94	116	-0.08	8.06	0.04
1986 05 07	TAM	1	105.96	8.02	7.97	213	-0.05	8.10	0.08
1986 05 07	TAM	2	254.04	8.02	7.96	80	-0.06	8.11	0.09
1986 05 07	WFM	1	63.59	8.02	7.88	256	-0.14	8.13	0.11
1986 05 07	WFM	2	296.41	8.02	7.98	142	-0.04	8.23	0.21
1986 07 09	KIP	1	75.69	6.20	6.51	183	0.31	6.31	0.11
1986 07 09	KIP	2	284.31	6.20	6.68	75	0.48	6.49	0.29
1986 07 09	PPT	1	84.72	6.20	6.35	64	0.15	7.07	0.87
1986 07 09	RER	1	72.92	6.20	6.64	256	0.44	6.43	0.23
1986 07 09	SCZ	1	106.31	6.20	6.44	213	0.24	6.30	0.10
1986 07 09	SCZ	2	253.69	6.20	6.45	80	0.25	6.33	0.13
1986 08 14	AGD	2	276.42	7.36	7.19	75	-0.17	7.70	0.34
1986 08 14	DRV	1	69.07	7.36	7.35	64	-0.01	7.52	0.16
1986 08 14	KIP	1	75.69	7.36	7.32	183	-0.04	7.38	0.02
1986 08 14	KIP	2	284.31	7.36	7.41	91	0.05	7.44	0.08
1986 08 14	NOC	1	45.46	7.36	7.32	183	-0.04	7.60	0.24
1986 08 14	NOC	2	314.54	7.36	7.35	91	-0.01	7.63	0.27
1986 08 14	PPT	1	84.63	7.36	7.38	64	0.02	7.94	0.58
1986 08 14	RER	1	72.91	7.36	7.27	213	-0.09	7.33	-0.03
1986 08 14	SCZ	1	106.36	7.36	7.42	98	0.06	7.46	0.10
1986 08 14	SCZ	2	253.64	7.36	7.29	213	-0.07	7.36	0.00

Table 4

GEOSCOPE Dataset

Event	Station	Passage	Δ	M_m^{pub}	M_m	T	r	M_c	r_c
1986 08 14	SSB	1	110.62	7.36	7.38	98	0.02	7.47	0.11
1986 08 14	SSB	2	249.38	7.36	7.27	107	-0.09	7.36	0.00
1986 08 14	TAM	1	117.66	7.36	7.32	98	-0.04	7.77	0.41
1986 08 14	TAM	2	242.34	7.36	7.30	107	-0.06	7.74	0.38
1986 08 14	WFM	1	131.75	7.36	7.33	64	-0.03	7.61	0.25
1986 08 14	WFM	2	228.25	7.36	7.09	75	-0.27	7.41	0.05
1986 10 14	AGD	1	111.30	6.18	6.62	75	0.44	6.47	0.29
1986 10 14	AGD	2	248.70	6.18	6.48	107	0.30	6.30	0.12
1986 10 14	KIP	1	54.24	6.18	6.25	256	0.07	6.57	0.39
1986 10 14	NOC	1	21.07	6.18	6.02	213	-0.16	6.58	0.40
1986 10 14	PPT	1	56.93	6.18	6.51	256	0.33	6.34	0.16
1986 10 14	WFM	1	123.32	6.18	6.26	98	0.08	6.58	0.40
1986 10 14	TAM	1	144.41	6.18	6.37	85	0.19	6.44	0.26
1986 10 20	DRV	1	46.75	7.65	8.06	183	0.41	7.73	0.08
1986 10 20	DRV	2	313.25	7.65	8.01	91	0.36	7.71	0.06
1986 10 20	KIP	1	52.48	7.65	8.01	256	0.36	7.68	0.03
1986 10 20	KIP	2	307.52	7.65	8.00	75	0.35	7.71	0.06
1986 10 20	NOC	1	16.74	7.65	8.10	213	0.45	7.73	0.08
1986 10 20	NOC	2	343.26	7.65	8.20	107	0.55	7.85	0.20
1986 10 20	PAF	1	82.68	7.65	7.89	80	0.24	7.85	0.20
1986 10 20	PAF	2	277.32	7.65	7.83	160	0.18	7.76	0.11
1986 10 20	PPT	1	26.82	7.65	7.96	213	0.31	7.73	0.08
1986 10 20	PPT	2	333.18	7.65	7.86	256	0.21	7.63	-0.02
1986 10 20	SSB	1	162.82	7.65	8.12	98	0.47	7.76	0.11
1986 10 20	SSB	2	197.18	7.65	8.07	213	0.42	7.69	0.04
1986 10 20	WFM	1	116.88	7.65	7.03	64	-0.62	7.66	0.01
1986 10 20	WFM	2	243.12	7.65	7.58	75	-0.07	8.20	0.55
1986 10 23	AGD	1	123.55	6.15	6.31	128	0.16	6.41	0.26
1986 10 23	KIP	1	48.47	6.16	5.84	67	-0.32	6.40	0.24
1986 10 23	NOC	1	11.21	6.16	6.39	213	0.23	6.57	0.41
1986 10 23	PPT	1	44.26	6.16	6.26	107	0.10	6.34	0.18
1986 11 14	AGD	1	75.43	7.11	7.52	91	0.41	7.47	0.36
1986 11 14	CAY	1	150.62	7.11	7.53	142	0.42	7.37	0.26
1986 11 14	CAY	2	209.38	7.11	7.29	80	0.18	7.15	0.04
1986 11 14	DRV	1	91.52	7.11	7.53	71	0.42	7.40	0.29
1986 11 14	DRV	2	268.48	7.11	7.58	107	0.47	7.44	0.33
1986 11 14	KIP	1	72.96	7.11	7.41	160	0.30	7.25	0.14
1986 11 14	KIP	2	287.04	7.11	7.29	213	0.18	7.13	0.02
1986 11 14	NOC	1	63.10	7.11	7.09	128	-0.02	7.34	0.23
1986 11 14	TAM	1	102.55	7.11	7.19	71	0.08	8.85	1.74
1986 11 14	TAM	2	257.45	7.11	7.03	80	-0.08	8.69	1.58
1986 11 14	WFM	2	248.09	7.11	7.43	98	0.32	7.48	0.37
1987 01 03	CRZ	1	96.12	6.08	6.43	80	0.35	6.28	0.20
1987 01 03	DRV	1	54.85	6.08	6.18	80	0.10	6.12	0.04
1987 01 03	KIP	1	49.34	6.08	6.26	183	0.18	6.13	0.05
1987 01 03	NOC	1	7.33	6.08	6.17	128	0.09	6.12	0.04
1987 01 03	PAF	1	83.64	6.08	6.39	128	0.31	6.24	0.16
1987 01 03	PPT	1	40.81	6.08	6.38	256	0.30	6.36	0.28
1987 01 03	SCZ	1	84.06	6.08	6.23	107	0.15	6.15	0.07
1987 01 03	WFM	1	120.27	6.08	6.23	183	0.15	6.15	0.07
1987 01 05	KIP	1	32.22	6.18	6.02	213	-0.16	6.56	0.38
1987 01 05	NOC	1	77.45	6.18	6.41	160	0.23	6.32	0.14
1987 01 05	PPT	1	71.96	6.18	5.98	183	-0.20	6.51	0.33
1987 01 05	SCZ	1	36.88	6.18	6.38	128	0.20	6.33	0.15
1987 01 05	WFM	1	60.20	6.18	6.34	71	0.16	6.80	0.62
1987 01 30	CAY	1	68.02	6.52	6.65	85	0.13	6.78	0.26
1987 01 30	CRZ	1	46.02	6.52	6.45	64	-0.07	6.81	0.29
1987 01 30	DRV	1	52.97	6.52	6.64	64	0.12	6.67	0.15
1987 01 30	KIP	1	128.44	6.52	6.48	213	-0.04	6.62	0.10
1987 01 30	NOC	1	97.14	6.52	6.58	213	0.06	6.78	0.26

Table 4

GEOSCOPE Dataset

Event	Station	Passage	Δ	M_m^{pub}	M_m	T	r	M_c	r_c
1987 01 30	SCZ	1	123.20	6.52	6.27	256	-0.25	6.55	0.03
1987 01 30	SSB	1	108.32	6.52	6.59	64	0.07	6.85	0.33
1987 02 06	KIP	1	54.00	6.11	6.24	256	0.13	6.26	0.15
1987 02 06	PPT	1	84.46	6.11	6.05	213	-0.06	7.00	0.89
1987 02 06	SCZ	1	73.78	6.11	6.34	256	0.23	6.30	0.19
1987 02 06	SSB	1	89.34	6.11	6.36	67	0.25	6.32	0.21
1987 02 06	TAM	1	107.52	6.11	6.29	67	0.18	6.36	0.25
1987 02 08	AGD	1	105.80	7.04	7.91	64	0.87	7.51	0.47
1987 02 08	AGD	2	254.20	7.04	7.64	128	0.60	7.23	0.19
1987 02 08	CAY	1	159.96	7.04	7.66	71	0.62	7.19	0.15
1987 02 08	CAY	2	200.04	7.04	7.57	213	0.53	7.09	0.05
1987 02 08	CRZ	1	89.79	7.04	6.83	256	-0.21	6.96	-0.08
1987 02 08	CRZ	2	270.21	7.04	6.80	256	-0.24	6.93	-0.11
1987 02 08	DRV	1	60.91	7.04	7.74	116	0.70	7.28	0.24
1987 02 08	KIP	1	59.70	7.04	7.47	98	0.43	7.09	0.05
1987 02 08	NOC	1	24.09	7.04	6.74	142	-0.30	6.85	-0.19
1987 02 08	PAF	1	77.42	7.04	7.09	64	0.05	7.43	0.39
1987 02 08	PPT	1	62.16	7.04	7.72	128	0.68	7.41	0.37
1987 02 08	PPT	2	297.84	7.04	7.67	98	0.63	7.36	0.32
1987 02 08	SCZ	1	94.17	7.04	7.18	160	0.14	6.93	-0.11
1987 02 08	SCZ	2	265.83	7.04	7.16	142	0.12	6.91	-0.13
1987 02 08	SSB	1	129.42	7.04	7.48	142	0.44	7.17	0.13
1987 02 08	SSB	2	230.58	7.04	7.49	80	0.45	7.18	0.14
1987 02 08	TAM	1	139.95	7.04	7.47	116	0.43	7.52	0.48
1987 02 08	TAM	2	220.05	7.04	7.40	142	0.36	7.45	0.41
1987 02 13	KIP	1	76.48	6.15	6.48	183	0.33	6.28	0.13
1987 02 13	KIP	2	283.52	6.15	6.62	75	0.47	6.45	0.30
1987 02 13	PPT	1	84.66	6.15	6.18	64	0.03	6.76	0.61
1987 02 13	SCZ	1	107.37	6.15	6.41	67	0.26	6.32	0.17
1987 02 13	SCZ	2	252.63	6.15	6.38	116	0.23	6.27	0.12
1987 02 13	SSB	1	111.23	6.15	6.62	91	0.47	6.52	0.37
		Additional Records for 1986 Aleutian Event							
1986 05 07	AGD	3	469.23	8.02	7.91	125	-0.11	8.09	0.07
1986 05 07	AGD	4	610.77	8.02	8.03	171	0.01	8.21	0.19
1986 05 07	AGD	5	829.23	8.02	7.96	107	-0.06	8.15	0.13
1986 05 07	CAY	3	465.52	8.02	7.83	284	-0.19	8.27	0.25
1986 05 07	CAY	4	614.48	8.02	8.11	284	0.09	8.55	0.53
1986 05 07	DRV	3	482.77	8.02	8.16	284	0.14	8.11	0.09
1986 05 07	DRV	4	597.23	8.02	8.02	213	0.00	7.97	-0.05
1986 05 07	DRV	5	842.77	8.02	8.24	151	0.22	8.19	0.17
1986 05 07	KIP	3	392.70	8.02	7.86	284	-0.16	8.34	0.32
1986 05 07	KIP	4	687.30	8.02	7.84	128	-0.18	8.31	0.29
1986 05 07	KIP	5	752.70	8.02	8.02	111	0.00	8.49	0.47
1986 05 07	NOC	3	435.28	8.02	8.03	284	0.01	7.98	-0.04
1986 05 07	NOC	4	644.72	8.02	7.90	197	-0.12	7.86	-0.16
1986 05 07	NOC	5	795.28	8.02	8.14	284	0.12	8.10	0.08
1986 05 07	PAF	3	499.78	8.02	8.06	107	0.04	8.54	0.52
1986 05 07	PAF	4	580.22	8.02	8.08	102	0.06	8.55	0.53
1986 05 07	PAF	5	859.78	8.02	8.14	135	0.12	8.69	0.67
1986 05 07	SSB	3	443.50	8.02	8.15	111	0.13	8.27	0.25
1986 05 07	SSB	4	636.50	8.02	7.94	111	-0.08	8.06	0.04
1986 05 07	SSB	5	803.50	8.02	8.05	256	0.03	8.16	0.14
1986 05 07	TAM	3	465.96	8.02	7.88	116	-0.14	8.01	-0.01
1986 05 07	TAM	4	614.04	8.02	7.89	160	-0.13	8.02	0.00
1986 05 07	TAM	5	825.96	8.02	8.03	284	0.01	8.15	0.13
1986 05 07	WFM	3	423.59	8.02	7.98	233	-0.04	8.22	0.20
1986 05 07	WFM	4	656.41	8.02	7.97	135	-0.05	8.19	0.17
1986 05 07	WFM	5	783.59	8.02	7.94	111	-0.08	8.16	0.14

Table 5

Averages and Standard Deviations of the Residuals r .

Dataset	Station Code	Number of Records	$\bar{r}$	σ	$\bar{r}_c$	σ_c
Whole dataset		307	0.12	0.29	0.19	0.25
Papeete	PPT	36	-0.13	0.34	0.02	0.25
GEOSCOPE		271	0.15	0.26	0.22	0.24
	Special Datasets					
Ten shortest distances		10	0.10	0.34	0.22	0.28
GEOSCOPE 1986 Aleutian		44	-0.05	0.13	0.17	0.19
[Rayleigh Waves From Paper I		256	0.14	0.25	0.09	0.19]
	Individual GEOSCOPE *Stations*					
Saint-Sauveur de Badole, France	SSB	46	0.15	0.28	0.19	0.24
Tamanrasset, Algeria	TAM	32	0.18	0.23	0.35	0.39
Pointe des Cafres, Réunion†	PCR,RER	31	0.10	0.23	0.16	0.22
Westford, Massachusetts	WFM	29	0.13	0.34	0.27	0.21
Port-aux-Français, Kerguelen Islands	PAF	18	0.11	0.19	0.29	0.21
Arga, Djibouti	AGD	22	0.25	0.31	0.19	0.14
Kipapa, Hawaii	KIP	20	0.10	0.28	0.14	0.12
Cayenne, French Guyana	CAY	19	0.19	0.25	0.17	0.11
Nouméa, New Caledonia	NOC	16	0.12	0.22	0.22	0.20
Santa Cruz, California	SCZ	12	0.13	0.15	0.07	0.10
Papeete, Tahiti	PPT	12	0.21	0.25	0.39	0.28
Dumont d'Urville, Antarctica	DRV	10	0.26	0.23	0.12	0.13
Crozet Island††	CRZ	4	-0.04	0.24	0.08	0.17

†We treat as a single dataset records from the Réunion Island station before and after it was moved (about 18 km) to Rivière de l'Est (RER) in 1986.

††Due to the small number of events, the values obtained at these stations may not be statistically significant.

We further define $r_c = M_c - \log_{10} M_0 + 20$. This formalism is identical to the path followed for Rayleigh waves in Paper I. Values of r_c are listed in the last columns of Tables 3 and 4. Statistical data on r_c are included in Table 5. For the GEOSCOPE dataset, the average amplitude of the focal correction was 0.26 unit, comparable to the case of Rayleigh waves (0.22), but its use resulted only in a meager reduction of the scattering, and actually in a significant deterioration of the average residual ($\bar{r} = 0.19$). We must conclude that in this case, the residuals r are not primarily due to ignoring exact focal parameters. They could be controlled by station noise, or involve energy propagating off the great-circle due to lateral heterogeneity. Indeed, a number of recent studies (MAUPIN, 1987; PAULSSEN *et al.*, 1989; TAJIMA and KAWASAKI, 1989) have evidenced significant Love wave polarization anomalies and instances of Love-Rayleigh coupling for individual sites and at higher frequencies. In particular, Figure 7 shows that some of the residuals r_c are very large; they correspond to measurements at the shorter end of the period range, and will be discussed in a later section.

On the other hand, in the case of PPT, the use of C_{FM} results in a spectacular improvement of the residuals, the average corrected residual being only $\bar{r}_c = 0.02$. This improvement is also apparent on Figure 7. A simple explanation is that most

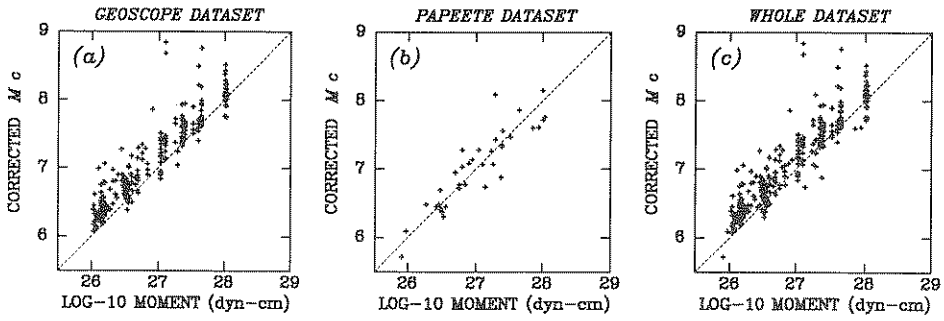

Figure 7
Same as Figure 6 for the corrected values M_c.

earthquakes used at PPT have their epicenters at the subduction zones surrounding the Pacific basin. This particular geometry means that PPT is most often at right angles from the strike of an event approaching a pure thrust-faulting mechanism ($\delta = 45°, \lambda = 90°$; referred to as "T45" in OKAL (1988)). This corresponds to a perfect node of Love wave excitation. It can be verified that even a geometry imperfect by 15° in any of the 3 angles results in a strong node at PPT, with a correction C_{FM} as large as 0.6–0.7 unit of magnitude.

Contrastingly, in the case of Rayleigh waves, and as discussed in detail by OKAL (1988), the isotropic term $K_0 s_R$ prevents the nodes of the radiation pattern from being fully developed (this term is excited by the biradial component M_{rr} in the moment tensor formalism). At low-frequency, and for a T45 source at depth h much smaller than the wavelength Λ, the shape of the radiation pattern takes the form $(-5/3 + \cos 2\phi)$, resulting in a maximum ratio of 4 (or ± 0.3 units of magnitude) between the amplitudes of nodes and lobes of radiation. The absence of this isotropic coefficient for Love waves allows the development of full-fledged nodes, which actually control the artificially low magnitudes observed at PPT. The central position of this station in the Pacific Basin generalizes the situation for most subduction zones, resulting in what could be described as a general site deficiency of Love waves.

Possible Influence of Distance

In this section, we examine systematically any possible correlation between the residuals r and the distance Δ at which the measurement is taken. Any systematic bias would suggest the use of an inadequate distance correction C_D, most probably in the form of poor Q models. Figure 8 plots the residuals r against Δ and shows that no significant trend exists in their population. When trying to regress r as a function of $\log_{10}\Delta$, a slope of only 0.048 is found for the GEOSCOPE dataset.

The PPT dataset exhibits very strong negative residuals in the 60–90° range, corresponding to earthquakes in the major circum-Pacific trenches. As explained

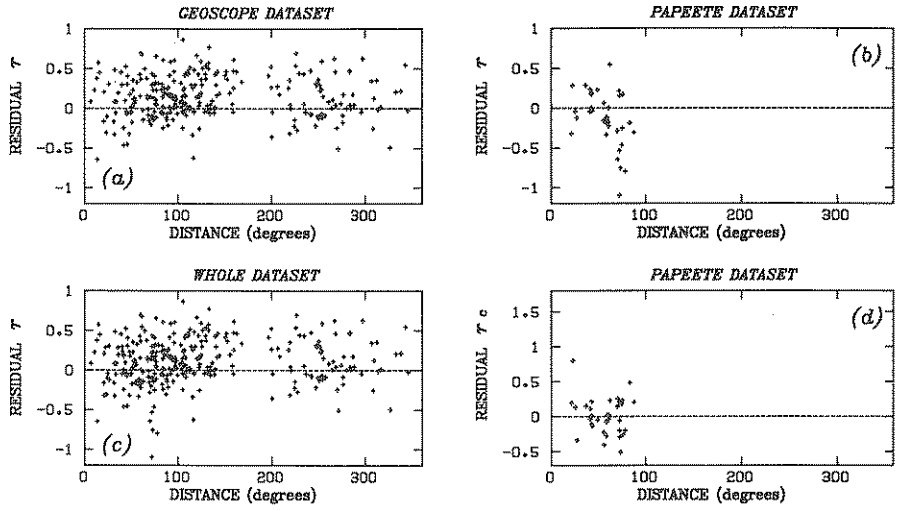

Figure 8
Residuals plotted as a function of distance Δ. (a, b, c): Residuals r for the GEOSCOPE, Papeete and whole datasets. In (d), the residuals are the corrected values r_c at PPT. Note that the strong anomalies present in (b) at 60–90° have disappeared.

above, this is an artifact of the particular focal mechanism geometries of these subduction zones in relation to the take-off azimuths to PPT. Indeed, if the corrected residuals r_c are plotted instead of r, this effect disappears, and no trend with distance is apparent (Figure 8d). Taken as a whole, the full dataset does not exhibit any trend of r as a function of Δ, and a slope of only 0.11 is achieved when regressing r against $\log_{10}\Delta$.

Extended Distances

In order to further explore the stability of the distance correction C_D, we targeted the 1986 Aleutian event for an extended study, gathering all available GEOSCOPE records, up to and including G_5. The largest distance involved was 860° or more than 95,000 km. Figure 9 shows a plot of r as a function of Δ in this extended range, and in particular shows the residual $r(n)$ for the n-th passage relative to $r(1)$ for the 1st passage at the same station. This procedure eliminates the possible contribution C_{FM} of focal mechanism and true depth. It is clear that no systematic trend exists even at the greatest distances sampled. We conclude that the corrections C_D, and in particular the Q models used in computing them, are adequate.

Dependence on Period

Figure 10 explores the possibility of a systematic dependence of r on period, which would indicate a flawed correction C_S. Again, no significant trend is present

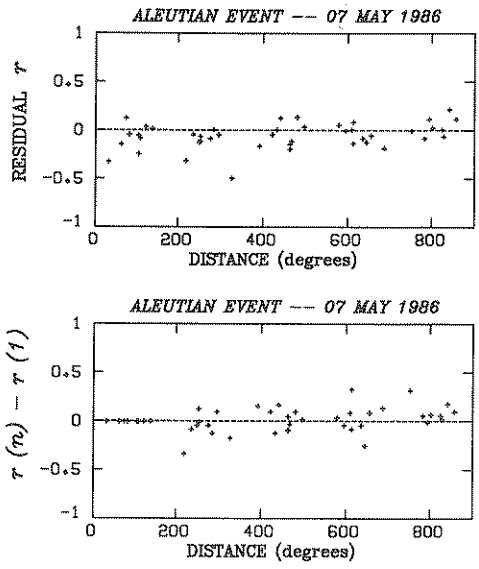

Figure 9

Residuals for the 36 GEOSCOPE records of the Aleutian event of 07 May 1986, up to and including G_5. *Top:* Raw residuals; *Bottom:* The residuals $r(1)$ of the first passage G_1 has been subtracted from the residual $r(n)$ of G_n at the same station.

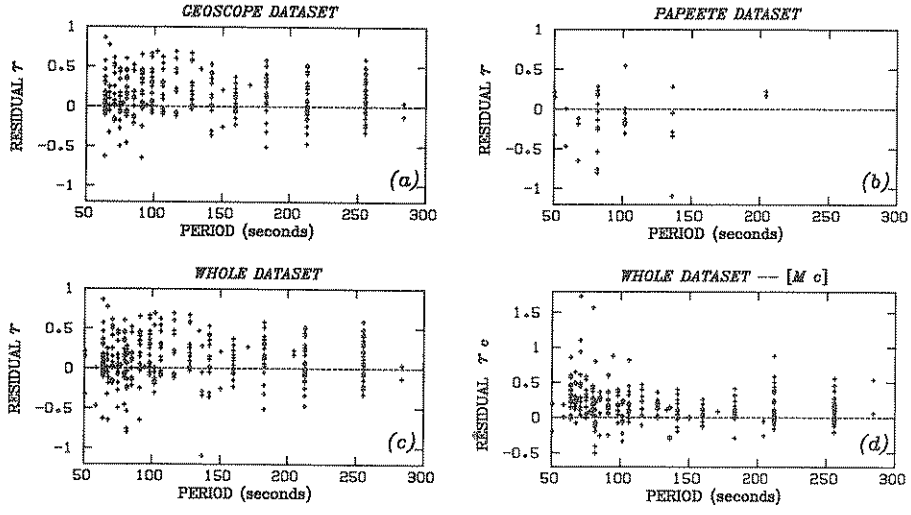

Figure 10

M_m residuals plotted as a function of the period T at which the measurement is retained. (a, b, c): Raw residuals r for each of the datasets. In (d), the residual plotted is the corrected r_c for the whole dataset. See text for details.

in any dataset, with a slope of at most 0.05 units of magnitude per octave (in the case of PPT). This number is comparable to that found in Paper I for Rayleigh waves. In general, the largest residuals are found at short periods (80 s and below), and this is especially true of the corrected residuals r_c (see Figure 10d). In two instances (the 1st and 2nd passages at TAM for the Taiwan earthquake of 14 November 1986), r_c reaches beyond 1.5 units of magnitude. In these cases, the focal correction C_{FM} is over 1.6 units. In other words, the station sits in an almost perfect node of radiation, and yet, significant energy is present. We interpret this as resulting either from an inaccurate focal mechanism, or more probably from Love energy traveling outside the great circle, due to lateral heterogeneity, a process most efficient at short periods. In such cases the magnitude approach yields a more accurate estimate of the seismic moment (or "size") of the event, since ignoring focal mechanism and true depth, in a sense compensates for also ignoring the effects of lateral heterogeneity. A similar conclusion was reached for Rayleigh waves, albeit with smaller residuals.

Possible Overtone Contamination

Another source of systematic errors at short periods could be the contamination of the spectrum by overtones.

We first investigated this question theoretically by computing the dispersion and excitation of the first 3 branches of overtones, in the period range 40–300 s, and for the PREM model. Results are shown on Figure 11. Around 50 s, all three branches have group velocities very close to that of the fundamental, leading to potential contamination. However, the third overtone branch ${}_3T_l$ becomes significantly faster around 60 s, ${}_2T_l$ around 80 s, and ${}_1T_l$ around 150 s. The bottom frames in Figure 11 show the logarithmic average excitabilities for the various branches at 25 and 75 km depth.

At 25 km depth, and for the first overtone branch, ${}_1L_{av}$ is always at least 0.55 units lower than ${}_0L_{av}$ for the fundamental; in other words, the overtone is excited at least 3.5 times less efficiently than the fundamental. In turns this means that the possible error on M_m due to contamination (for an average focal mechanism) is no more than 0.15 units of magnitude. The contribution of the higher branches, ${}_2T_l$ and ${}_3T_l$ is even smaller: ${}_2L_{av}$ is about 0.75 units smaller than ${}_0L_{av}$, suggesting a maximum error of 0.09 units of M_m, and ${}_3L_{av}$ a full unit below ${}_0L_{av}$, contributing at most 0.05 units to M_m. In principle, one could expect a maximum error of 0.29 units in a worst case scenario requiring all interferences to be constructive. This would be possible only at the shortest periods, since as T grows, the higher overtone branches propagate at faster group velocities and cease to be contaminant. An error of ± 0.15 unit is probably more realistic in the range 50–80 s.

As shown in Figure 11c these results are not expected to be significantly changed over the range of depths considered in the present study. However, for intermediate

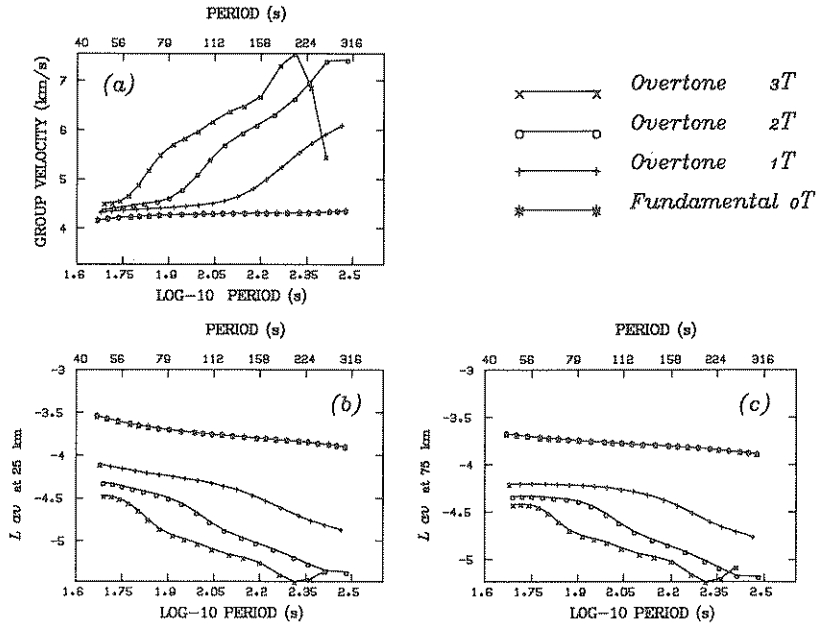

Figure 11

Potential influence of overtone contamination on M_m: (a) Group velocity as a function of period for the fundamental and first three Love overtone branches, ${}_pT_l$, $p = 0, 1, 2, 3$. (b, c): Logarithmic average excitability at 25 and 75 km compared for the four branches.

and deep earthquakes, overtone excitation becomes comparable to, if not larger than, that of fundamentals. Because of the similarity in group velocities, the resulting contamination rules out any attempt to extend the mantle magnitude M_m to Love waves at those depths, as we successfully did for Rayleigh waves (OKAL, 1990).

For the purpose of studying the possible influence of this problem in detail, we reprocessed all the data, in the narrower period range $T \geq 80$ s. This resulted in an average change in M_m of -0.09 unit for the 72 values in Tables 3 and 4 measured at periods less than 80 s. As shown in the statistics on Table 6, the restriction in period does not improve the quality of fit; in most instances, it actually deteriorates the standard deviations.

In this respect, we failed to evidence any serious overtone contamination of the measured mantle magnitude M_m. This reflects the fact that even contamination by an overtone with 20–30% of the fundamental's amplitude affects the measured magnitude by only 0.2 units, a figure comparable to the general precision of our measurements. On the other hand, a similar overtone, if in quadrature of phase with the fundamental, can introduce as much as 15–20° of error in the phase

Table 6

Averages and Standard Deviations of the Residuals r with Periods Constrained to $T \geq 80$ s.

Dataset	Station Code	Number of Records	$\bar{r}$	σ	$\bar{r}_c$	σ_c
Whole dataset		307	0.10	0.30	0.17	0.25
Papeete	PPT	36	-0.17	0.37	-0.03	0.24
GEOSCOPE		271	0.13	0.27	0.20	0.24
Special Datasets						
Ten shortest distances		10	0.09	0.34	0.23	0.28
GEOSCOPE 1986 Aleutian		44	-0.06	0.14	0.17	0.19
Individual GEOSCOPE *Stations*						
Saint-Sauveur de Badole, France	SSB	46	0.13	0.27	0.17	0.22
Tamanrasset, Algeria	TAM	32	0.16	0.23	0.33	0.38
Pointe des Cafres, Réunion†	PCR,RER	31	0.08	0.24	0.15	0.21
Westford, Massachusetts	WFM	29	0.09	0.36	0.23	0.21
Arga, Djibouti	AGD	22	0.23	0.31	0.17	0.12
Kipapa, Hawaii	KIP	20	0.09	0.29	0.13	0.13
Cayenne, French Guyana	CAY	19	0.16	0.26	0.16	0.11
Port-aux-Français, Kerguelen Islands	PAF	18	0.10	0.20	0.28	0.22
Nouméa, New Caledonia	NOC	16	0.12	0.22	0.22	0.20
Santa Cruz, California	SCZ	12	0.13	0.14	0.06	0.10
Papeete, Tahiti	PPT	12	0.19	0.27	0.38	0.27
Dumont d'Urville, Antarctica	DRV	10	0.21	0.28	0.08	0.13
Crozet Island††	CRZ	4	-0.06	0.24	0.07	0.16

†We treat as a single dataset records from the Réunion Island station before and after it was moved (about 18 km) to Rivière de l'Est (RER) in 1986.

††Due to the small number of events, the values obtained at these stations may not be statistically significant.

information, a figure often significant, especially at long periods. This example stresses the generally robust character of magnitude measurements.

Test at 10 Shortest Distances

Within the framework of a tsunami warning, it is particularly important to assess the performance of M_m at very short distances, at which an immediate estimate of an earthquake's moment is of crucial importance to the issuance of tsunami warnings or alerts (TALANDIER and OKAL, 1989). For this purpose, we repeated the experiment carried out for Rayleigh waves by isolating and studying separately the records with the 10 shortest distances, ranging in this case from 7.33° to 22.72°. Most of them involve the Pacific stations NOC and PPT for events at the Solomon, Vanuatu and Samoa trenches. The data, compiled as part of Table 5, and also presented on Figure 12, demonstrate that the performance and accuracy of M_m in providing a real-time estimate of the size of an event is unchanged at short distances. In particular, there is no deterioration of the accuracy of M_m for events with very large moments, which could entice significant tsunami danger.

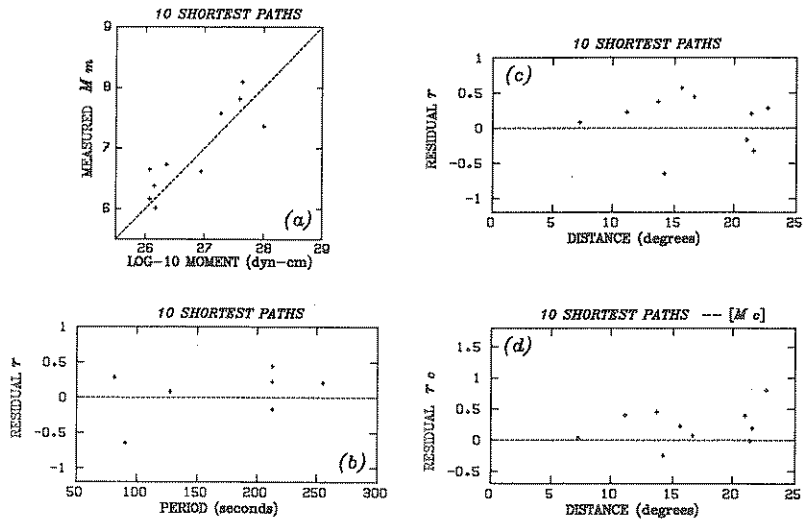

Figure 12
Performance of M_m for the 10 shortest paths. (a) is similar to Figure 6; (b) to Figure 10; and (c) and (d) to Figures 8a and 8d, respectively.

Comparison with Rayleigh Residuals and Combined Use of the Two Waves

We compare in this section the performance of the two magnitude scales, for those cases when measurements were taken both on Rayleigh and Love waves, at the same station for the same events.

The intersection of the two datasets comprises 31 events at Papeete and 96 GEOSCOPE paths, or 49% of the combination of the two datasets. This seemingly low number partially reflects the different time windows used in the two studies by virtue of operational constraints (e.g., many GEOSCOPE records for 1986 and 1987 were available only after the completion of the Rayleigh study). Figures 13 and 14 are plots of the Rayleigh and Love residuals, respectively for the PPT and GEOSCOPE datasets. In general, Rayleigh residuals are found to be smaller in amplitude than the corresponding Love residuals. A statistical analysis reveals that the Rayleigh and Love datasets are poorly correlated, with correlation coefficients of 0.33 for GEOSCOPE data and 0.20 at PPT. In particular, there is no evident anticorrelation of Rayleigh and Love residuals, as would be expected from the influence of focal geometry in the case of "pure" focal mechanisms, for which Rayleigh and Love radiation patterns are mutually conjugate. This is probably a reflection of the relatively small number of strike-slip mechanisms, and of the prominence of mechanisms approaching the T45 geometry. Furthermore, the corrected residuals r_c^R and r_c^L do not correlate any better (correlation coefficients are 0.15 for GEOSCOPE and 0.06 at PPT), indicating that the origin of the residuals r_c is not related simply to the path from epicenter to station.

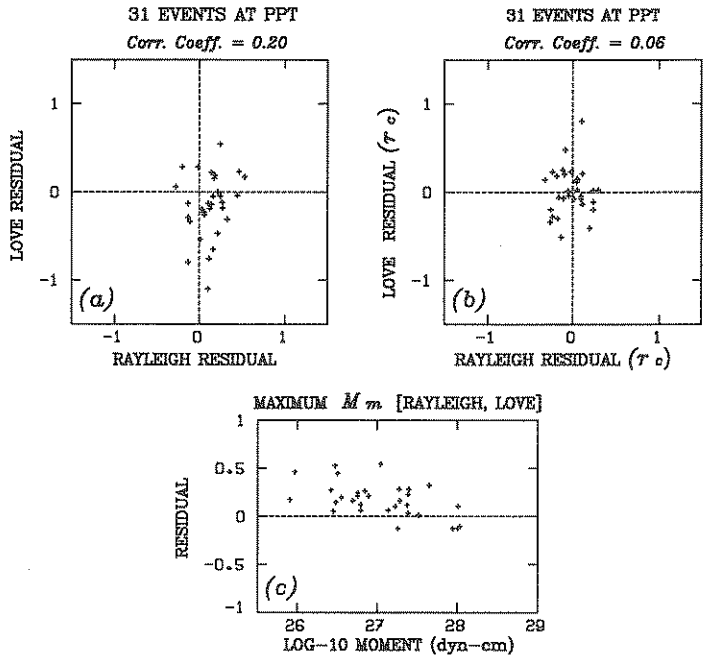

Figure 13
Comparison of Rayleigh and Love residuals for events common to the two studies at PPT. (a) and (b): Raw and corrected residuals r and r_c, respectively; (c): Residual r obtained by retaining the largest of the two M_m values for Rayleigh and Love waves.

In addition, Figures 13 and 14 show that in general, the procedure of retaining the maximum among M_m^R and M_m^L provides an adequate safeguard against underestimating significantly the seismic moment of the event. The only exceptions to this pattern correspond to stations lying along a strike from a thrust faulting event approaching the T45 geometry: WFM for the 1985 Chilean earthquake, and CAY for the 1985 Mexican and 1986 Aleutian events. This does not constitute a particularly dangerous situation in itself, since for each observatory, considered as isolated, the location and focal geometries of the relevant earthquakes can be identified in advance, and an *ad hoc* focal correction effected.

Station Corrections?

Finally, the data in Table 5 illustrate that individual station residuals are usually between 0.10 and 0.20 units of magnitude. As in the case of Rayleigh waves, the largest station residuals $\bar{r}$ (at AGD and DRV) are artifacts of the focal geometry of the particular events involved. Figure 15 shows that there is no significant correlation between the average Love and Rayleigh residuals at individual stations, either for raw residuals $\bar{r}$ (correlation coefficient 0.10) or for the corrected residuals $\bar{r}_c$

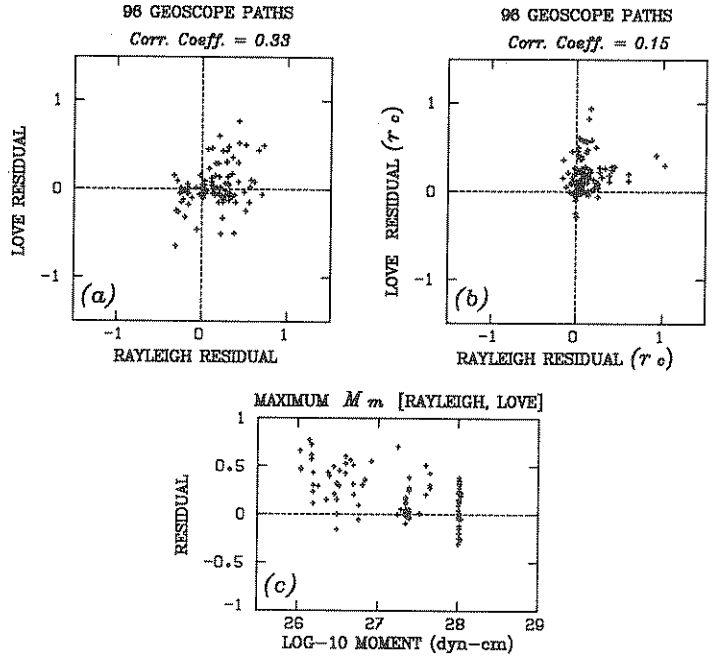

Figure 14
Same as Figure 13 for the GEOSCOPE dataset.

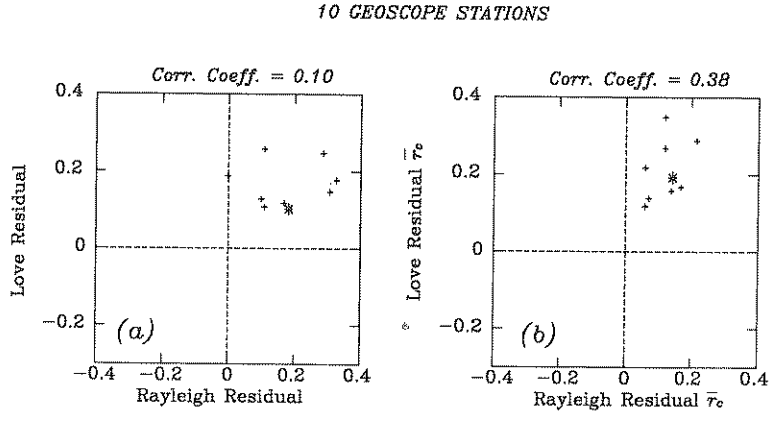

Figure 15
Comparison of average Rayleigh and Love residuals at individual GEOSCOPE stations (see Table 5). (a): Raw residuals $\bar{r}$; (b): Corrected residuals $\bar{r}_c$. On each frame, the larger asterisk indicates two stations with identical sets of Love and Rayleigh residuals.

(correlation coefficient 0.38). The concept of a "station correction" to either or both of the magnitude scales is not warranted. This is not surprising since the very long wavelengths used for M_m average out the structural heterogeneities which could be expected to control station corrections at shorter periods.

5. Conclusion

We have shown that it is possible to develop a Love wave version of the mantle magnitude M_m, based on the use of Equations (3), (4) and (7). Based on the analysis of a dataset of more than 300 Love phases, we have verified the adequacy of the corrections C_S and C_D. The performance of the resulting values of M_m is comparable to that of the Rayleigh scale defined in Paper I. In particular, because the period at which the measurement is taken is not fixed, this Love wave mantle magnitude avoids the saturation at high moments characteristic of the classical scales such as M_s.

In general, the residuals are somewhat more scattered than for Rayleigh waves, and this is at least partly due to the effect of radiation patterns, which are more pronounced for Love waves because of the absence of an isotropic term excited by the biradial component of the moment tensor M_{rr}. Contamination with overtones is found to be largely negligible at periods greater than 50 s, in view of the general precision of the measurements. When both Rayleigh and Love waves are used, the larger of the two magnitudes M_m^R and M_m^L in general guards against underestimation of the seismic moment by more than 0.15 units of magnitude. The only exceptions are in extremely particular focal geometries, such as a station along a strike from a pure thrusting event on a 45° dipping fault.

Acknowledgements

We are grateful to Barbara Romanowicz for providing a regular flow of GEOSCOPE data. Michael Wysession assisted with statistical software. John Woodhouse and his colleagues provided computerized datasets of centroid moment tensor solutions in advance of publication. This research was supported by Commissariat à l'Energie Atomique (France), and the National Science Foundation under Grant Number EAR-87-20549.

References

BOORE, D. M. (1969), *Effect of Higher Mode Contamination on Measured Love Wave Phase Velocities*, J. Geophys. Res. *74*, 6612–6616.

CANAS, J., and MITCHELL, B. J. (1978), *Lateral Variation of Surface-wave Anelastic Attenuation Across the Pacific*, Bull. Seismol. Soc. Am. *68*, 1637–1650.

CARA, M. (1978), *Regional Variations of Higher Rayleigh-mode Phase Velocities: A Spatial Filtering Method*, Geophys. J. Roy. Astr. Soc. *54*, 439–460.

DZIEWONSKI, A. M., and ANDERSON, D. L. (1981), *Preliminary Reference Earth Model*, Phys. Earth Planet. Inter. *25*, 297–356.

DZIEWONSKI, A. M., FRIEDMAN, A., GIARDINI, D., and WOODHOUSE, J. H. (1983a), *Global Seismicity of 1982: Centroid Moment-tensor Solutions for 308 Earthquakes*, Phys. Earth Planet. Inter. *33*, 76–90.

DZIEWONSKI, A. M., FRIEDMAN, A., and WOODHOUSE, J. H. (1983b), *Centroid Moment-tensor Solutions for January–March 1983*, Phys. Earth Planet. Inter. *33*, 71–75.

DZIEWONSKI, A. M., FRANZEN, J. E., and WOODHOUSE, J. H. (1983c), *Centroid Moment-tensor Solutions for April–June 1983*, Phys. Earth Planet. Inter. *33*, 243–249.

DZIEWONSKI, A. M., FRANZEN, J. E., and WOODHOUSE, J. H. (1984a), *Centroid Moment-tensor Solutions for July–September 1983*, Phys. Earth Planet. Inter. *34*, 1–8.

DZIEWONSKI, A. M., FRANZEN, J. E., and WOODHOUSE, J. H. (1984b), *Centroid Moment-tensor Solutions for October–December 1983*, Phys. Earth Planet. Inter. *34*, 129–136.

DZIEWONSKI, A. M., FRANZEN, J. E., and WOODHOUSE, J. H. (1984c), *Centroid Moment-tensor Solutions for January–March 1984*, Phys. Earth Planet. Inter. *34*, 209–219.

DZIEWONSKI, A. M., FRANZEN, J. E., and WOODHOUSE, J. H. (1985a), *Centroid Moment-tensor Solutions for April–June 1984*, Phys. Earth Planet. Inter. *37*, 87–96.

DZIEWONSKI, A. M., FRANZEN, J. E., and WOODHOUSE, J. H. (1985b), *Centroid Moment-tensor Solutions for July–September 1984*, Phys. Earth Planet. Inter. *38*, 203–213.

DZIEWONSKI, A. M., FRANZEN, J. E., and WOODHOUSE, J. H. (1985c), *Centroid Moment-tensor Solutions for October–December 1984*, Phys. Earth Planet. Inter. *39*, 147–156.

DZIEWONSKI, A. M., FRANZEN, J. E., and WOODHOUSE, J. H. (1985d), *Centroid Moment-tensor Solutions for January–March 1985*, Phys. Earth Planet. Inter. *40*, 249–258.

DZIEWONSKI, A. M., FRANZEN, J. E., and WOODHOUSE, J. H. (1986a), *Centroid Moment-tensor Solutions for April–June 1985*, Phys. Earth Planet. Inter. *41*, 215–224.

DZIEWONSKI, A. M., FRANZEN, J. E., and WOODHOUSE, J. H. (1986b), *Centroid Moment-tensor Solutions for July–September 1985*, Phys. Earth Planet. Inter. *42*, 205–214.

DZIEWONSKI, A. M., FRANZEN, J. E., and WOODHOUSE, J. H. (1986c), *Centroid Moment-tensor Solutions for October–December 1985*, Phys. Earth Planet. Inter. *43*, 185–195.

DZIEWONSKI, A. M., EKSTRÖM, G., FRANZEN, J. E., and WOODHOUSE, J. H. (1987a), *Global Seismicity of 1979; Centroid Moment-tensor Solutions for 524 Earthquakes*, Phys. Earth Planet. Inter. *48*, 18–46.

DZIEWONSKI, A. M., FRANZEN, J. E., and WOODHOUSE, J. H. (1987b), *Centroid Moment-tensor Solutions for January–March 1986*, Phys. Earth Planet. Inter. *45*, 1–10.

DZIEWONSKI, A. M., EKSTRÖM, G., FRANZEN, J. E., and WOODHOUSE, J. H. (1987c), *Centroid Moment-tensor Solutions for April–June 1986*, Phys. Earth Planet. Inter. *45*, 229–239.

DZIEWONSKI, A. M., EKSTRÖM, G., FRANZEN, J. E., and WOODHOUSE, J. H. (1987d), *Centroid Moment-tensor Solutions for July–September 1986*, Phys. Earth Planet. Inter. *46*, 305–315.

DZIEWONSKI, A. M., EKSTRÖM, G., WOODHOUSE, J. H., and ZWART, G. (1987e), *Centroid Moment-tensor Solutions for October–December 1986*, Phys. Earth Planet. Inter. *48*, 5–17.

DZIEWONSKI, A. M., EKSTRÖM, G., FRANZEN, J. E., and WOODHOUSE, J. H. (1988a), *Global Seismicity of 1981; Centroid Moment-tensor Solutions for 542 Earthquakes*, Phys. Earth Planet. Inter. *50*, 155–182.

DZIEWONSKI, A. M., EKSTRÖM, G., WOODHOUSE, J. H., and ZWART, G. (1988b), *Centroid Moment-tensor Solutions for January–March 1987*, Phys. Earth Planet. Inter. *50*, 116–126.

DZIEWONSKI, A. M., EKSTRÖM, G., WOODHOUSE, J. H., and ZWART, G. (1988c), *Centroid Moment-tensor Solutions for April–June 1987*, Phys. Earth Planet. Inter. *50*, 215–225.

DZIEWONSKI, A. M., EKSTRÖM, G., WOODHOUSE, J. H., and ZWART, G. (1988d), *Centroid Moment-tensor Solutions for July–September 1987*, Phys. Earth Planet. Inter. *53*, 1–11.

DZIEWONSKI, A. M., EKSTRÖM, G., WOODHOUSE, J. H., and ZWART, G. (1989), *Centroid Moment-tensor Solutions for October–December 1987*, Phys. Earth Planet. Inter. *54*, 10–21.

FORSYTH, D. W. (1975), *A New Method for the Analysis of Multi-mode Surface-wave Dispersion; Application to Love Wave Propagation in the East Pacific*, Bull. Seismol. Soc. Am. *65*, 323–342.

FURUMOTO, M., and FUKAO, Y. (1976), *Seismic Moments of Great Deep Shocks*, Phys. Earth Planet. Inter. *11*, 352–357.

GELLER, R. J. (1976), *Scaling Relations for Earthquake Source Parameters and Magnitudes*, Bull. Seismol. Soc. Am. *66*, 1501–1523.

GILBERT, J. F., and DZIEWONSKI, A. M. (1975), *An Application of Normal Mode Theory to the Retrieval of Structural Parameters and Source Mechanism from Seismic Spectra*, Phil. Trans. Roy. Soc. London *278A*, 187–269.

HARKRIDER, D. G. (1964), *Surface Waves in Multi-layered Media. I: Rayleigh and Love Waves from Buried Sources in a Multilayered Half-space*, Bull. Seismol. Soc. Am. *54*, 627–679.

HWANG, H.-J., and MITCHELL, B. J. (1987), *Shear Velocities, Q_β, and the Frequency Dependence of Q_β in Stable and Tectonically Active Regions from Surface Wave Observations*, Geophys. J. R. Astr. Soc. *90*, 575–613.

KANAMORI, H. (1970), *Velocity and Q of Mantle Waves*, Phys. Earth Planet. Inter. *2*, 259–275.

KANAMORI, H., and STEWART, G. S. (1976), *Mode of Strain Release along the Gibbs Fracture Zone, Mid-Atlantic Ridge*, Phys. Earth Planet. Inter. *11*, 312–332.

MAUPIN, V., *Etude des caractéristiques des ondes de surface en milieu anisotrope; application à l'analyse d'anomalies de polarisation à la station de Port-aux-Français*, Thèse, (Université Louis Pasteur, Strasbourg 1987).

MITCHELL, B. J., and YU, G.-K. (1980), *Surface-wave Dispersion, Regionalized Velocity Models, and Anisotropy of the Pacific Crust and Upper Mantle*, Geophys. J. R. Astr. Soc. *63*, 497–514.

NAKANISHI, I. (1981), *Shear Velocity and Shear Attenuation Models Inverted from the World-wide and Pure-path Average Data of Mantle Rayleigh Waves ($_0S_{25}$ to $_0S_{80}$) and Fundamental Normal Modes ($_0S_2$ to $_0S_{24}$)*, Geophys. J. R. Astr. Soc. *66*, 83–130.

OKAL, E. A. (1988), *Seismic Parameters Controlling Far-field Tsunami Amplitudes: A Review*, Natural Hazards *1*, 67–96.

OKAL, E. A. (1989), *A Theoretical Discussion of Time-domain Magnitudes: The Prague Formula for M_s and the Mantle Magnitude M_m*, J. Geophys. Res. *94*, 4194–4204.

OKAL, E. A. (1990), *M_m: A Variable-period Mantle Magnitude for Intermediate and Deep Earthquakes*, Pure Appl. Geophys. *134*, 333–354.

OKAL, E. A., and GELLER, R. J. (1979), *On the Observability of Isotropic Seismic Sources: The July 31, 1970 Colombian Earthquake*, Phys. Earth Planet. Inter. *18*, 176–196.

OKAL, E. A., and JO, B.-G. (1983), *Regional Dispersion of First-order Overtone Rayleigh Waves*, Geophys. J. Roy. Astr. Soc. *72*, 461–481.

OKAL, E. A., and TALANDIER, J. (1989), *M_m: A Variable Period Mantle Magnitude*, J. Geophys. Res. *94*, 4169–4193.

PAULSSEN, H., LEVSHIN, A. L., SNIEDER, R., and LANDER, A. V. (1989), *Anomalous Surface Wave Polarization in the Iberian Peninsula as Inferred from ILAHA Data*, Proc. XXVth Gen. Assemb. Int. Assoc. Seismol. Phys. Earth's Inter., Istanbul, Aug. 21–Sept. 1, 1989, p. 526 [abstract].

ROMANOWICZ, B., CARA, M., FELS, J.-F, and ROULAND, D. (1984), *GEOSCOPE: A French Initiative in Long-period Three-component Global Seismic Networks*, Eos, Trans. AGU *65*, 753–754.

TAJIMA, F., and KAWASAKI, I. (1989), *3-D Particle Motion Trajectories: Direct Observation of Love-Rayleigh Coupling*, Geophys. Res. Letts. *16*, 1051–1054.

TALANDIER, J., and OKAL, E. A. (1989), *An Algorithm for Automated Tsunami Warning in French Polynesia, Based on Mantle Magnitudes*, Bull. Seismol. Soc. Am. *79*, 1177–1193.

THATCHER, W., and BRUNE, J. N. (1969), *Higher Mode Interference and Observed Anomalous Apparent Love Wave Phase Velocities*, J. Geophys. Res. *74*, 6603–6611.

(Received October 9, 1989, accepted May 1, 1990)